CLONAL ANALYSIS OF NEOCORTICAL GLIOGENESIS

A Dissertation

Presented to the Faculty of the Weill Cornell Graduate School

of Medical Sciences

In Partial Fulfillment of the Requirements for the Degree of

Doctor of Philosophy

by

Luisirene Hernandez

August 2018

CLONAL ANALYSIS OF NEOCORTICAL GLIOGENESIS

Luisirene Hernandez, PhD

Cornell University 2018

Proper neural function relies on the regulation of the diversity and the proportion of neuronal and non-neuronal cell types. Glia, non-neuronal neural cells, have emerged as key players in the development, function, and maintenance of the central nervous system (CNS). Glia constitute as much as 50% of the cellular population in the CNS. As our understanding of the array of glial functions increases, little is understood about the physiological basis and developmental origin of glial abundance and diversity.

`

The mammalian neocortex is a highly organized structure that plays a crucial role in higher-order brain functions such as cognition and integrating sensory input. Radial glial progenitors (RGPs) that line the cerebral ventricles and are positive for the transcription factor *Emx1* produce neocortical excitatory neurons and glia in a sequential manner. Previous lineage tracing has revealed that at the conclusion of neurogenesis 16% of RGPs proceed to gliogenesis. During development, these RGPs

generate discrete columnar structures that contain neurons, astrocytes, and oligodendrocytes. To understand how the diversification of glia is mediated by individual progenitors, we performed clonal analysis of neocortical RGPs at their transition from neurogenesis to gliogenesis using Mosaic Analysis with Double Markers (MADM).

In terms of lineage specification, our analysis uncovered three distinct types of gliogenic RGPs based on their potential to generate neural cell types. The proportion RGP subtypes is independent of time of exit from neurogenesis and location along the anterior-posterior axis. Quantitatively, MADM-based clonal analysis of neocortical gliogenesis revealed that the number of glia produced by an individual RGP is independent from the time exit from neurogenesis occurs. Our analysis shows that the overall ratio of *Emx1*-derived glia to neurons is 1:5. Our analysis suggests that although the majority of neocortical astrocytes are *Emx1*-RGP derived, a significant proportion of oligodendroglia are derived from other origins. We also found that different programs regulate the proliferation of astrocyte-restricted and oligodendrocyte-restricted glial precursors, with oligodendrocyte precursors having a larger proliferative capacity compared to astrocyte precursors. In terms of distribution and structure, analysis of the laminar distribution of astrocyte clones suggests separate lineages for Layer-1 and

white matter (WM) astrocytes and that astrogliogenesis, similar to neurogenesis, proceeds in an inside-out fashion. Most oligodendrocyte clones are clustered into a single layer and the majority of RGP-derived oligodendrocytes are destined for deep cortical layers, whereas RGP-derived astrocytes are more evenly spread through the cortical width. Our results reveal how the production of neuronal and non-neuronal cell types are developmentally regulated in individual progenitors. In particular, shedding insight on the regulation of lineage specification of glial types, establishment of neuron:glia ratio, and the distribution and structure of RGP-derived glia in the neocortex.

BIOGRAPHICAL SKETCH

Luisirene Hernandez was born in New York City and brought up in Santo Domingo, Dominican Republic. She attended The City College of New York where she obtained her Bachelor's degree of Science in Biochemistry in 2012. Her first research experience was in the laboratory of Dr. Marco Ceruso at the City College of New York where she applied computational biophysics to study protein conformational changes upon ligand binding. As her interest in neuroscience grew, she joined the laboratory of Dr. Itzhak Mano in the Sophie Davis School of Biomedical Education during her junior year. There she studied glutamate clearance and excitotoxicity using the nematode *C. elegans* as a model system. After graduating City College, she joined the laboratory of Dr. David Raizen in the University of Pennsylvania as part of the PennPREP Post-baccalaureate program. There she constructed *C. elegans* models to study neurological and sleep disorders.

At the conclusion of her time in the University of Pennsylvania in 2012, Luisirene enrolled in the graduate program in neuroscience at Weill Cornell Graduate School of Medical Sciences in New York City. She joined the laboratory of Dr. Song-Hai Shi in the Department of Developmental Biology at Memorial Sloan Kettering Cancer Center for

her dissertation work, where she studied neurogenesis and gliogenesis in the murine neocortex.

ACKNOWLEDGEMENTS

There are an infinite number of people I need to thank for their support, although the word thankful is an understatement compared to my degree of gratitude. Firstly, I thank my research advisor and mentor Dr. Song-Hai Shi who has been extraordinarily patient, understanding, supportive, and invaluable in his guidance. Without his wisdom, faith, and his necessary "nudges" to persevere, I would not have come this far.

I am also grateful to all members of the Shi lab, past and present, for their help and support over the years. It is my privilege to have worked with all of you. Thank you for creating a work environment that encourages the pursuit of excellence in research. You are all an inspiration for me to give my best. I especially thank Kate Peng Gao for her indispensable help with the MADM experiments. I would also like to thank Zhizhong Li for his openness to help with techniques and laboratory resources. I am also grateful for the administrators who have offered a lot of support throughout my graduate study; Lily Erdy, Sonia Das, Cara Monaco, and Susan Lin. I would like to extend this gratitude to members of the Joyner, Kaltschmidt, and Goll labs for their support over the years and for creating an enjoyable work environment on the 7th floor.

I would especially like to acknowledge my committee members Dr. Costantino Iadecola, Dr. Natalia De Marco Garcia, and Dr. Anna Orr for your thoughtful advice and constant support throughout my PhD. I am extremely fortunate to have your guidance in developing my research project and in the process of preparing this dissertation.

I am grateful to all members of the Weill Cornell Neuroscience graduate program, especially Dr. Elizabeth Ross for her continued support since the start of my time in Weill. I would also like to thank Dr. Heidi Stuhlmann in the Department of Cell and Developmental Biology of Weill Cornell, for encouraging my interest in developmental biology and fostering an excitement for the subject.

I would like to thank my previous mentors, Dr. Marco Ceruso, Dr. Itzhak Mano, and Dr. David Raizen for introducing me to scientific research and neuroscience. Thank you for inspiring me to pursue my academic goals. I would also like to thank the MARC/RISE programs (Minority Access to Research Careers/Research Initiative for Scientific Enhancement) and CCAPP (City College Academy for Professional Preparation) at City College of New York for their invaluable support and guidance,

especially Dr. Jonathan Levitt, Dr. Millicent Roth, and Nkem Stanley I would also like to thank Dr. Jean Boyer, Dr. Hillary Nelson, and Dr. Arnaldo Diaz from PennPREP (Postbaccalaureate Research Education Program) at the University of Pennsylvania for their aid in preparing for graduate school and a research career. I want to thank all my classmates and laboratory colleagues from my pre-doctoral training for being my company and support through this journey into academic research.

Most importantly, I would like to express my deepest gratitude to my family for the unconditional love and support, especially my parents, Martha Rodriguez and Luis Hernandez, my grandmother Gladys Soriano, and my sister Marylis Hernandez, who have always believed in me and encouraged me to follow my dreams. I want to thank my aunts and uncles, Pedro Ovalle, Ramona Arias, Austria Rodriguez, Norma Lopez, Teodulo Lopez, Ingrid Mejia, Mary Nova, and Ramona Mentor for their invaluable support throughout my education. I want to thank God for giving me the faith to keep towards my goals.

This work was partially supported by NIH T32 grant support (T32-HD060600) awarded to LH.

TABLE OF CONTENTS

LIST OF FIGURES

LIST OF ABBREVIATIONS

3D ..... three-dimensional
A ..... anterior
ASD ..... autism spectrum disorder
ATP ..... adenosine tri-phosphate
BMP ..... bone morphogenetic protein
CGE ..... caudal ganglionic eminence
CNS ..... central nervous system
CNTF ..... ciliary neurotrophic factor
CT-1 ..... cardiotrophin 1
D ..... dorsal
E ..... embryonic day
eGFP ..... enhanced green fluorescent protein
GAT3 ..... GABA transporter type 3
GFAP ..... glial fibrillary acidic protein
GFP ..... green fluorescent protein
GLAST ..... glutamate aspartate transporter
Gli-1 ..... Zinc finger protein GL1, glioma-associated oncogene
GLYT1 ..... glycine transporter 1
GM ..... gray matter
IPC ..... intermediate progenitor cell
JAK-STAT ..... Janus kinase signal transducer and activator of transcription
Kir4.1/*KCNJ10* ..... ATP-sensitive inward rectifier potassium channel 10
L ..... layer
LGE ..... lateral ganglionic eminence
LIF ..... leukemia inhibitory factor
MADM ..... Mosaic analysis with double markers
MARCM ..... Mosaic analysis with a repressible cell marker
MBP ..... myelin basic protein
MGE ..... medial ganglionic eminence
MOG ..... myelin oligodendrocyte glycoprotein
mPFC ..... medial prefrontal cortex
MS ..... multiple sclerosis
N+A ..... neuron and astrocyte
N+A+O ..... neuron, astrocyte, and oligodendrocyte
NFIA ..... Nuclear factor 1 A-type
N+O ..... neuron and oligodendrocyte

NPC ..... neural progenitor cell
OPC ..... oligodendrocyte precursor cell
P ..... posterior
P ..... postnatal day
PLP ..... proteolipid protein
PNS ..... peripheral nervous system
RGP ..... radial glial progenitor
RFP ..... red fluorescent protein
Sc-RNAseq ..... single-cell RNA sequencing
SVZ ..... subventricular zone
TBR2 ..... T-box brain protein 2
tdTomato ..... tandem dimer Tomato
TM ..... tamoxifen
V ..... ventral
VZ ..... ventricular zone
WM ..... white matter

Chapter 1

Introduction to gliogenesis in the neocortex

1.1 Neural cells of the cerebral cortex.

Proper neural function requires the generation of diverse neuronal and glial cell types in correct proportions. Glia is a term that refers to the non-neuronal cells of the nervous system and comprises several cell types including microglia, ependymal cells, astrocytes, and oligodendrocytes in the central nervous system (CNS); and Schwann cells and satellite cells in the peripheral nervous system (PNS). Classically considered a homogenous passive population that has a mere support role, glia are increasingly recognized to be key players in neural development, function, and maintenance. Glia play many roles which include supplying nutrients to neurons, and providing structural support to neural tissue; they insulate and repair axons, clear the extracellular environment of pathogens and dead neurons, and regulate synaptogenesis and synaptic transmission. Despite the wide array of functions assigned to glia, and the fact that they constitute about 50% of the cellular population in the brain[1,2], our understanding of glia

function, physiology, and development has greatly lagged behind that of their neuronal counterparts.

The physiological basis and developmental origin of glial abundance and heterogeneity persists as an open question. Although there is evidence for physiological, morphological, and molecular diversity in glial populations, the origins and functional implications of this heterogeneity are poorly understood, in great part due to the lack of tools to study specific astrocyte subpopulations. A deeper understanding of glial development may reveal novel cell fate determinants for glia and provide tools for the manipulation of specific subpopulations. This will allow a deeper interrogation of glial contribution during development, how they maintain proper brain function, how they malfunction in disease, and how they repair tissue. In addition, because glia retain their capacity to proliferate and differentiate during adulthood, novel therapies may be developed that take advantage of glial developmental and repair processes to regenerate neural cells and tissue.

A significant hindrance to the study of glial function and properties has been the lack of tools to specifically target glial progenitors and glial subpopulations. We circumvent this limitation by focusing our study of gliogenesis on a specific neural

progenitor cell (NPC) population, the radial glia progenitor (RGP) of the telencephalic dorsal ventricular zone which produces excitatory neurons and glia of the neocortex in a sequential manner. Through the study of a common precursor of neurons and glia, we venture to explore the impact of developmental origin in the assembly of the neural population of the neocortex. Our work reveals how the proper number of neural cells, subtypes, and their distribution are regulated by individual RGPs

The balance between the number of neuronal and non-neuronal cells is evolutionarily constrained suggesting a close link between neurogenesis and gliogenesis. Although the neuron-glia ratio varies across species, brain regions, and possibly disease contexts, the scaling rules that describe the relationship between neurons and glia vary uniformly with neuronal density across mammalian species spanning 90 years of evolution[1]. This evolutionary constraint suggests a regulation of the mechanisms controlling glial development. This leads us to hypothesize that neurogenesis and gliogenesis are tightly coupled at the single progenitor cell level. To test this hypothesis, I aim to systematically analyze the potential of individual progenitors in generating neurons and glial cells. Our data reveals previously unknown mechanisms for specification of different neural cell types from common progenitors *in vivo*.

1.2 Neocortical glial subtypes

The following subsections are an overview of the macroglia of the neocortex – astrocytes and oligodendrocytes. We focus our study on these glial cell types since they are derived from a common RGP progenitor along with neurons. Although microglia are the other prominent glial population in brain, they are not the topic of this study. Microglia do not originate from the neuroepithelium, as do the other neural cell types; but originate in the yolk sac, invading the neuroepithelium of the developing brain around E9.5, prior to the establishment of the blood-brain barrier[3].

1.2.1 Astrocytes and their functional diversity

Astrocytes are stellate cells that branch into numerous processes that are in intimate association with surrounding synapses and vasculature. Astrocytes are thus positioned to be active participants in neural processes such as lactate metabolic coupling[4], regulation of cerebral blood flow[5], and synapse formation[6] and synaptic transmission[7–9].

The close association of astrocytes to both pre- and post-synaptic components of neurotransmission has led to the coining of the term "tripartite synapse" to refer to the integration of these three elements in the modulation of synaptic transmission[10].

Astrocytes regulate levels of neurotransmission through the clearing of neurotransmitters from the synaptic cleft. Although their ability to modulate synaptic transmission through the release of "gliotransmitters" remains controversial, astrocytes express diverse types of receptors for different neurotransmitters. Following an increase of intracellular calcium, astrocytes release gliotransmitters such as glutamate[11], ATP[12], and D-Serine[13,14]. Astrocytes are homogenously distributed within the grey matter occupying non-overlapping territories so that the neuronal parenchyma is divided into territories of similar volumes termed "synaptic islands" where an estimated 100,000 synapses are under the regulation of a hippocampal astrocyte, and 600-800 under the regulation of a neocortical astrocyte[15,16]. Astrocytes may also communicate extensively with each other via gap junction-mediated calcium signaling[17]. Normal astrocytic activity is important for cognitive function. For instance, astrocytic activity and Ca^{2+} signaling are necessary for motor learning[18]. Astrocyte dysfunction has been implicated in conditions such as schizophrenia, autism spectrum disorder (ASD), and Fragile X syndrome[19–21].

Astrocytes are key mediators of neurovascular coupling. Cerebral blood flow is modulated in response to neural activity to meet the metabolic needs of neurons in a process termed functional hyperemia[22]. This provides neurons increased levels of

oxygen and glucose while helping clear excess metabolites and neurotransmitters from the extracellular space. Neurons rarely make direct contact with the vasculature, relying instead on astrocytes as intermediaries for communication with the cerebral vasculature. Electron microscopy shows perivascular processes of astrocytes completely ensheath the endothelial cells in the blood vessels of the cerebral microvasculature; astrocyte endfeet interdigitate extensively at vascular endfoot-endfoot contacts, with little discontinuity between[23]. Most protoplasmic astrocytes extend at least one perivascular endfoot. A specialized subtype of astrocyte, the perivascular astrocyte, has been described which has its soma in direct contact with the cerebral vasculature. Clonal analysis of cortical astrocytes after *in utero* electroporation at E14 using the Star Track approach, which relies on the stochastic expression of 12 different fluorescent reporters under the control of the *hGFAP* promoter, revealed clones composed of up to 40 perivascular astrocytes distributed radially along a single blood vessel[24]. This suggests that perivascular astrocytes in the cortex are derived from a common progenitor. Perivascular astrocytes have been observed to preferentially proliferate compared to surrounding protoplasmic (gray matter) astrocytes in response to cortical injury– a response that is clone-specific[25,26].

1.2.2 Neocortical astrocyte heterogeneity

Little is known about whether astrocytes encode heterogeneous signals involved in neuronal circuit formation and/or maintenance. There is a clear morphological distinction between astrocytes in different brain regions[27]. Molecularly, single-cell RNA-sequencing (sc-RNAseq) revealed seven subclasses of astrocytes with distinct regional allocations. These subtypes differ in the expression of several genes including neurotransmitter transporters such as GAT3 (GABA transporter type 3) and GLYT1 (glycine transporter 1), which may confer distinct physiological properties between subtypes. Astrocyte subpopulations throughout the brain could be further subdivided based on GFAP expression (high versus low). Astrocytes from the two pools of GFAP-expression are molecularly similar, suggesting GFAP expression is a source of variability independent from the previously mentioned seven subclasses identified by scRNAseq [28]. Although there is increasing data on interregional differences between astrocytes, there is limited evidence of heterogeneity among astrocytes dispersed in the same region, particularly in terms of function and molecular expression. In the telencephalon, two subtypes of astrocytes were identified by sc-RNAseq which differ in the expression of several genes[28]. Heterogeneity in *Gli-1* (Zinc finger protein GL1, glioma-associated oncogene) expression has been described in cortical astrocytes[29]; in the human brain, a subpopulation of astrocytes expresses the cell adhesion molecule CD44[30]; in the hippocampus, Kir4.1(*KCNJ10*/ATP-sensitive inward rectifier potassium

channel 10) expression differs among the astrocyte population, resulting in heterogeneity in hippocampal astrocyte physiological properties[31].

The current established astrocyte subtypes of the mammalian neocortex are distinguished by morphological and location criteria. They also differ in the amount of GFAP detectible by immunohistochemistry. In the murine brain, these subtypes are: (1) protoplasmic astrocytes – this cell type has a stellate morphology with 5-6 main branches radiating from the cell soma and branches into smaller ramifications, granting them a "bushy" appearance. Protoplasmic astrocytes are distributed throughout the gray matter. (2) Fibrous astrocytes – characterized by their localization in the white matter, have thick branching processes with a higher expression level of the intermediate filament glial fibrillary acidic protein (GFAP) than protoplasmic astrocytes[32]. (3) There are specialized astrocytes in layer I of the neocortex which cover the surface just under the pia mater, forming the glial limiting membrane or *glia limitans*. Evidence suggests that layer 1 astrocytes may have a different developmental origin than the two aforementioned subtypes. They are characterized by having a "fibroblast-like" morphology and high expression of GFAP[24,26]. Two additional astrocyte subtypes are exclusive to primate brains: (4) interlaminar astrocytes, whose cells bodies reside in Layer 1 and extend straight processes terminating in blood vessels

in layers 2-4[33]. (5) The second primate-exclusive astrocyte subtype are the varicose projection astrocytes which are situated mainly in layers 5 and 6 and extend one to five processes up to 1 mM long which may terminate in the vasculature or neuropil[34].

1.2.3 Overview of oligodendrocytes and NG2-cells

Oligodendrocytes are responsible for the myelination of axons, providing the physical and physiological insulation that allows for the saltatory conduction of signals along axons: Myelinated segments lack voltage-gated ion channels, preventing the loss of electrical signal along the axon. Unmyelinated segments, termed nodes of Ranvier, are enriched for voltage-gated sodium channels. Current generated by an action potential travels from one node of Ranvier through myelinated segments, where myelin prevents current from leaking across the internodal membrane. When the current reaches the node of Ranvier in the next segment, voltage-gated channels open and regenerate the action potential. Action potentials therefore jump from one unmyelinated segment to the next, hence the term "saltatory" conduction. Saltatory conduction accelerates the velocity at which electrical signal travels the axons. Myelinated axons can conduct to velocities up to 150m/s, compared to 0.5-10 m/s for unmyelinated axons[35]. CNS oligodendrocytes form myelin sheaths on multiple axons,

up to 30, so that sequential myelinated segments on an axon are derived from different oligodendrocytes. Myelin is an extension of the plasma membrane of oligodendrocytes and has a composition high in lipids, including sphingomyelin and cholesterol. It's also composed proteins such as myelin basic protein (MBP), myelin oligodendrocyte glycoprotein (MOG), and proteolipid protein (PLP) which provide myelin with structural integrity.

Skill learning is associated with an increase in myelination in axonal tracts of relevant circuits. This proliferation may be mediated through increased neural activity as it has been demonstrated that stimulation of neurons promotes oligodendrogenesis and increases myelination in a circuit-specific manner[36]. The conductance of action potentials is modulated by the width of the myelin sheath and internodal distance. Although myelination is crucial to brain function and demyelination is a feature of many neurological diseases including multiple sclerosis (MS), the mechanisms for myelination and axon recognition by oligodendrocytes are not well understood. In addition to providing axonal insulation, oligodendrocytes also provide critical trophic and metabolic support to neurons[37].

The adult CNS also contains an abundant population of oligodendrocyte precursor cells (OPCs). These cells, positive for the chondroitin-surface proteoglycan 4 (*cspg4*/NG2) are termed NG2-cells, and their specialized functions beyond acting as OPCs have led to their recognition as the fourth major glial population in the CNS, distinct from oligodendrocytes, astrocytes, and microglia. Like astrocytes, these cells are distributed throughout the gray matter and maintain unique territories via self-avoidance. Loss of an NG2-cell through death, differentiation to oligodendrocytes, or ablation, leads to the proliferation of adjacent cells. These cells also proliferate in response to injury to participate in tissue repair, or activity to mediate myelination. NG2-cells are distributed uniformly throughout different neocortical layers even though oligodendrocyte density is significantly higher in the deep layers. This suggests that many NG2 cells never differentiate into oligodendrocytes[38]. Despite being recognized as OPCs, NG2-cells also have the potential to generate astrocytes in the ventral forebrain during development, but not at adult stages[39].

1.2.4 Neocortical oligodendrocyte heterogeneity

Oligodendrocytes have been considered a functionally homogenous population in the CNS. However, single-cell RNA sequencing revealed thirteen distinct populations of oligodendrocytes representing a continuum from *Pdgfra*+ OPCs to distinct mature

oligodendrocytes[40]. There is more evidence of functional heterogeneity in NG2 cells (OPCs). NG2-cells have heterogeneous differentiation potential – NG2 cells of the ventral, but not the dorsal, forebrain have the potential to generate astrocytes. These ventral NG2 glia generate gray matter (GM) (protoplasmic) but not WM (fibrous) astrocytes[39,41]. In the dorsal cortex, GM and WM NG2 cells differ in their electrophysiological properties[42]. In adult mice, GM NG2 cells mostly generate post-mitotic NG2-cells, whereas WM NG2-cells generate mostly mature oligodendrocytes[43].

Current criteria for distinction between subtypes of oligodendrocytes would require sc-RNAseq or *in situ* hybridization to distinguish between different oligodendrocytes. Clonal analysis requires very sparse labeling of progenitors and the resulting daughter cells, so we are unable to combine this method with our MADM approach to examine how developmental origin may contribute to oligodendrocyte heterogeneity. In contrast, for astrocytes, we may use morphology and laminar location to identify their subtype.

1.3 The Radial Unit Hypothesis

The mammalian neocortex is a highly organized structure that plays a crucial role in higher-order brain functions such as cognition and integrating sensory input. The radial

unit hypothesis, postulated in 1988 by Pasko Rakic, suggests that the RGP-derived ontogenetic column is the basic building block of the cerebral cortex[44,45].

The hallmarks of neocortical structural and functional organization are lamination and radial organization. Evidence supports that the behavior of the RGP underlies the formation of this highly ordered structure. The neocortex is a six-layered structure, the boundaries of which can be readily distinguished by histological staining. Each layer has unique neuronal populations with distinct morphology, molecular composition, and afferents and projections, which links cytoarchitecture to function. These ordered laminae are formed through a concerted production and migration of neurons[46]. Thus, a single RGP progenitor proceeds to diversify the neuronal population of the cortex through sequential derivation of different subtypes through a common progenitor, and cell number is generated by a deterministic program where each progenitor generates 8-9 neurons[47].

1.3.3 Sequential derivation of neural cell subtypes from a common RGP

In the developing neocortex, neurons and three types of macroglia – astrocytes, NG2-cells, and oligodendrocytes, are derived from common multipotent NPCs. In the earliest stages of neurodevelopment, the neural tube is composed of a single layer of

neuroepithelial cells (NE). As development proceeds, around E9, a more fate-restricted progenitor is specified from the NE, the radial glial progenitor (RGP). RGPs reside in the transient ventricular zone (VZ) which lines the cerebral ventricles. RGPs are characterized by their bipolar morphology, with a short apical process which acts as an end foot anchorage to the VZ surface, and a basal process that extends to the pial surface. At early stages of neurogenesis, RGPs divide symmetrically to expand the progenitor pool, and then switch to asymmetric division where they self-renew and generate one daughter cell: either a post-mitotic neuron or an intermediate progenitor cell (IPC). IPCs may undergo one to two rounds of symmetric division in the subventricular zone (SVZ) to generate neurons. Generated neurons migrate along the radial glial fiber. Early-born neurons migrate to the nascent cortical plate; successive waves of neurons migrate past earlier born neurons occupying increasingly superficial layers[48–56]. At the conclusion of neurogenesis, around E16, RGPs proceeds to gliogenesis. It would be of interest to examine whether the similar processes that lead to the diversification of the neuronal population also contribute to generating the diverse glial subtypes of the neocortex.

1.3.2 Role of RGP in the functional assembly of the neocortex

Functionally, the neocortex is organized into functional columns so that neurons sharing common properties, for instance receptive fields in somatosensation or orientation selectivity in vision, are distributed radially so that these properties are similar between neurons within a column but differ significantly among adjacent columns[57].

Lineage relationship plays an important role in the functional organization of the cortex. It has been suggested that the RGP-derived ontogenetic column is related to functional columns. Previous work has found that lineage-related sister neurons preferentially form chemical synapses with each other. This preferential coupling is in part mediated by preferential gap-junction coupling of sister cells[58,59]. To support this hypothesis, it has been demonstrated that sister excitatory neurons in layer 2/3 exhibit similar orientation tuning properties[60]. Because neurons and glia are derived from the same RGP pool, how does the lineage relationship influence the number, subtypes, and functional relationships of glia and neurons?

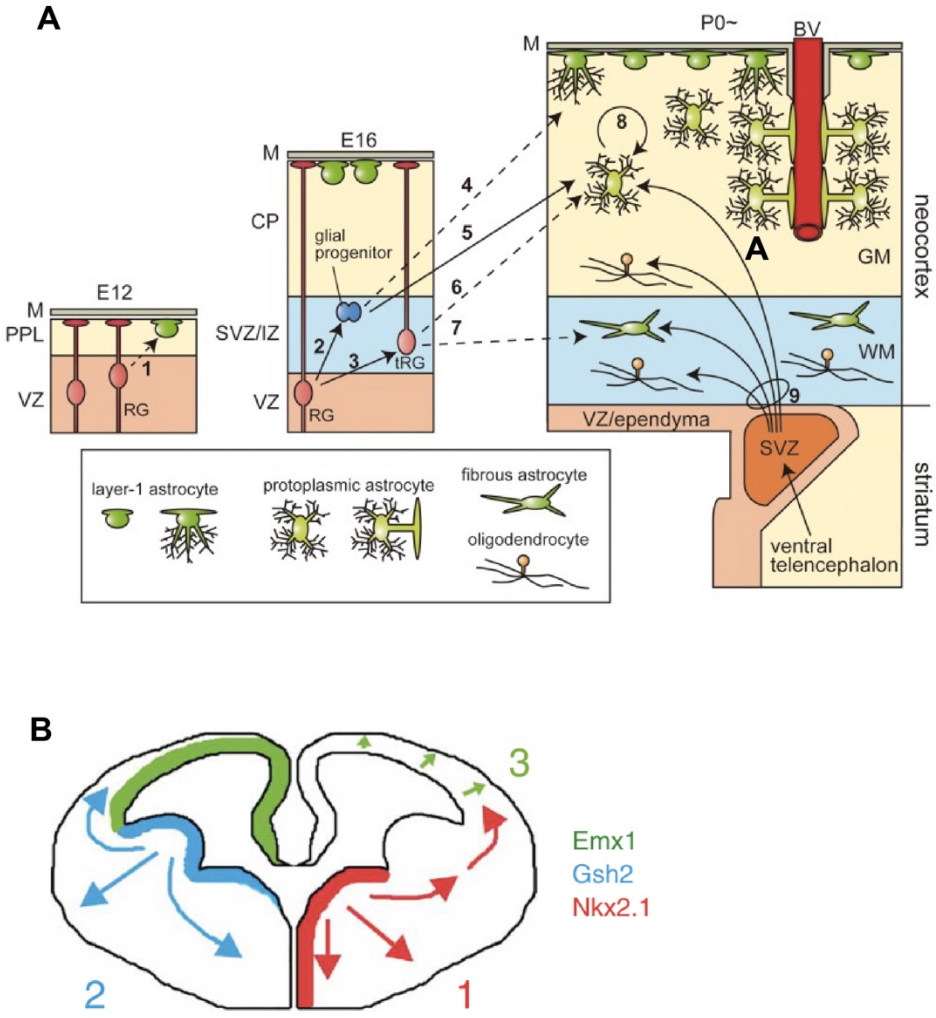

Figure 1.1. Diverse of origins of neocortical glia. (A) Various modes of astrogliogenesis and astrocyte subtypes. Image panels represent astrocyte generation during different developmental stages. Different modes of division are described in the following subsections: mode 1, section 1.6.1; mode 2, section 1.6.3; mode 3, section 1.6.2; mode 4, section 1.6.4; mode 5-8, section 1.6.5. E, embryonic day; P, postnatal day; GM, gray matter; WM, white matter; M, meninges or pia matter; PPL, primordial plexiform layer; VZ, ventricular zone; SVZ, subventricular zone; IZ, intermediate zone; CP, cortical plate; BV, blood vessel. Adapted from Tabata, 2015[61]. (B) Three different waves of competing oligodendrocytes derived from different progenitor domains. Wave 1, from Nkx2.1-expressing progenitors in the MGE VZ starting at E12.5; wave 2, from Gsh2-expressing progenitors in the LGE-CGE VZ starting at E15.5; wave 3, Emx1-expressing progenitors starting around birth. Adapted from Kessaris et. al 2006[62].

1.4 The neuron/glia switch in RGPs

Temporal control of the switch from neurogenesis to gliogenesis is critical to producing numbers and subtypes of neural cells in correct proportions to sustain brain function. The mechanism controlling the transition from neurogenesis to gliogenesis in the vertebrate CNS is complex and not well understood. The gliogenic switch occurs around E12.5 in the spinal cord and E16 in the cortex. In the murine brain, RGPs are first exclusively GLAST+/Nestin+ and produce neurons preferentially (GLAST: glutamate aspartate transporter). A population of GLAST+/Nestin- RGPs emerges in the later stages, that preferentially produces astrocytes[63]. In rodents, RGPs are GFAP-negative until the completion of neurogenesis, where the intermediate filament protein composition is switched from vimentin to GFAP[45].

Our understanding of glial development is hindered by the lack of markers to exclusively target glial-specific progenitors. Most current evidence for astroglial-specific transcription factors in mammals has come from studies in the developing spinal cord. NFIA (Nuclear factor 1 A-type) was found to be both necessary and sufficient for embryonic gliogenesis as well as astrogenesis[64]. Sox9 was also shown to regulate early gliogenesis through its regulation of NFIA induction and its association with NFIA during subsequent gliogenic stages[65,66]. NFIA is expressed in OPCs and antagonizes the

ability of Sox10 to induce myelin genes, with the level of NFIA being downregulated before myelin gene expression. Overexpression and knock-down experiments *in vitro* and *in vivo* suggest that Zbtb20, together with Sox9 and NFIA, promotes astrocytogenesis[67].

In our understanding of gliogenesis, the link between astrogliogenesis and oligodendrogenesis remains unclear. The existence Zbtb20+/Olig2+ cells that are negative for Sox10, a marker of OPCs, has been reported[67]. This suggests that cells expressing Olig2 may act as astrocyte precursors. It is unclear whether these Olig2+ astroglial progenitors have lost or will gain Sox10 expression to transition to or from oligodendrogenesis. At the population level, neocortical astrocytes are detected at earlier timepoints than oligodendrocytes.

Astrogliogenesis begins towards the end of the neurogenic period and is regulated by cell-intrinsic programs as well as extrinsic signals that decrease neurogenic and increase astrogenic competence over developmental time. Intrinsic programs include epigenetic changes that lead to Polycomb-dependent suppression of proneural genes such as the neurogenins *ngn1* and *ngn2*[68]. Extrinsic signals include leukemia inhibitory factor (LIF), ciliary neurotrophic factor (CNTF), and cardiotrophin-1 (CT-1), which are

members of the interleukin-6 family of cytokines. Cytokine signaling activates the JAK-STAT (Janus kinase – signal transducer and activator of transcription) pathway which promotes astrocyte differentiation[69,70]. In addition, bone morphogenic protein (BMP)-Smad and Notch signaling pathways engage in cross-talk with the JAK-STAT pathway to promote astrocyte differentiation[71].

1.5 Three different competing waves of oligodendrocytes

Oligodendrocytes of the telencephalon are generated in three temporally and spatially distinct waves: The first wave appears at E12.5 and originates from *Nkx2.1*+ progenitors in the medial ganglionic eminence (MGE). The second wave appears at E15.5, in the lateral ganglionic eminence (*Gsh2*+ progenitors). The third wave arises at P0 from the cerebral cortex (*Emx1*+ progenitors). OPCs derived from the first two waves migrate tangentially to populate the cortex, where cells from one wave are selectively lost and replaced by OPCs from the subsequent waves[62]. The mechanisms for this oligodendrocyte loss are unknown. Death may be due to the competition for survival signal from axons[72] but how oligodendrocytes from one particular domain selectively pruned is not yet understood (Figure 1.1B).

In the neocortex, NG2 cells from the last two cohorts (*Gsh2, Emx1*) are intermingled creating a mosaic population in respect to domain of origin. OPCs reach peak density during the first postnatal week, after which their density declines and their processes become less overlapping but begin to occupy defined domains throughout the entire parenchyma. At early postnatal stages, the contribution of cortical OPCs is about 30% from *Gsh2* and 70% from *Emx1*. However, the latter population drops to 30% as postnatal development proceeds[62].

Although distinct origins may lead to NG2 subtype heterogeneity, evidence suggests that cells derived from different domains are equivalent/similar or at least plastic enough to replace each other: direct ablation of NG2-cells generated during one of the waves could be completely compensated by cells originating from the other neural precursors[62].

The relative contribution of radial glia and SVZ progenitors to NG2 cell/oligodendrocyte production is not well established. It is also not known whether and how the astrogliogenesis program is suppressed when NG2 cells are generated or whether all progenitor cells in the pallium are equivalent in their ability to produce both astrocytes and NG2-cells after neurogenesis has been completed.

1.6 Diverse origins of cortical astrocytes

During CNS development, neurogenesis precedes gliogenesis, with radial glia serving as both the scaffolding and the neural stem cell (NSC) for both cell types. During the first three weeks of postnatal development, the glial cell population expands 6-8-fold in the rodent brain[73]. However, during early postnatal stages, radial glial cells lose their basal processes after they exit neurogenesis. This suggests different mechanisms generating the second wave of astrocytes (Figure 1.1A). There have been five routes of astrogenesis described.:

1.6.1 Dividing RGP in the VZ:

Lineage tracing studies in the spinal cord (SC) suggest that mature astrocyte populations are "tethered" to their VZ site of origin, suggesting limited migration during development[74]. Glia may be derived directly from a dividing RGP or be produced via an astrocyte-restricted precursor. Although studies have demonstrated the existence of astrocyte and glia-specific precursors[75], specific markers for these cells remain largely uncharacterized.

1.6.2 Transformation of RGPs:

The telencephalic RGPs are transient, and disappear or transform into astrocytes with the completion of cortical development. The differentiation of transforming RG to astrocytes has been directly shown by live-imaging[54]. RGP apical process retracts and RGP becomes multipolar in morphology resembling an astrocyte. However, direct transformation of RG may only produce a limited number of astrocytes. Most radial glia have finished producing their share of astrocytes and have begun to disappear shortly after birth.

1.6.3 Intermediate Glial Progenitors in SVZ:

Classic lineage tracing experiments have established that astrocytes, in great part, derive from progenitors at the SVZ at early postnatal stages. SVZ progenitors and the production of astrocytes from proliferative glial progenitors in the SVZ almost ends by P14[76].

1.6.4 Marginal zone/L1 astrocyte precursors:

In an early wave of astrocyte production, around the stage when the pre-plate forms, a subset of VZ-derived cells move on to the basal lamina underlining the pia mater and differentiate into Layer-1 astrocytes and form the subpial glia limiting membrane. As development proceeds, astrocytes, likely derived from the SVZ, migrate

into layer 1 to join the earlier generated astrocytes. It is not clear whether these different origins correspond to different subtypes of astrocytes, namely the fibroblast-like and protoplasmic astrocytes, since both reside in layer 1. In support of this hypothesis, clones of protoplasmic and clones of fibroblast-like astrocytes in Layer-I appeared to be exclusive of each other[24], as demonstrated by lineage tracing using the technique StarTrak. Star Trak relies on the combinatorial expression of 12 distinct fluorescent proteins under the regulation of the hGFAP promoter. Marginal zone/L1 progenitors are not exclusive to making L1 astrocytes: it has been reported that a subset of protoplasmic astrocytes arises from Layer-I astrocytes or multipotent progenitors in layer-I of the cerebral cortex, so protoplasmic astrocytes may be derived from layer 1 progenitors, not just progenitors in the SVZ.[32,77].

1.6.5 Local proliferation of differentiated astrocytes:

Local generation of astrocytes within the postnatal cortex is thought to be a major source of glia, at least in layers I-IV, whereas astrocytes early in development are derived from radial glia and SVZ progenitors. While electroporation of P0-2 pups showed that only 3% of astrocytes derived postnatally from SVZ progenitors reached layer I-IV, local low titer retrovirus injections in superficial cortical layers at P0-2 and analysis 7-10 days later showed that as much as 50% of astrocytes had been generated

from local divisions. Symmetric division of differentiated astrocytes was confirmed by two-photon imaging.[78] This finding has led to the notion that astrocyte population expansion is based on 'pioneer' astrocytes – astrocytes derived from VZ/SVZ can migrate to colonize layers and then proliferate by local division.

1.6 Previous *in vivo* lineage tracing of neocortical neural progenitors in vivo

Genetic tracing methods of progenitors have also found a developmental relationship between neurons and glia. Neural progenitors in the neocortex generate discrete columnar structures that contain both projection neurons and protoplasmic astrocytes. Using a Thy1.2 Cre mouse line in which a random sparse subset of neural progenitors undergoes CRE/lox recombination, the astrocyte to neuron ratio of labeled cells in a labeled column was 1:7.4, similar to the overall ratio of 1:8.4 across the entire gray matter of the neocortex. This indicates that column-associated astrocytes account for the majority of astrocytes in the neocortex. Dividing cells were found at the base of neuronal columns at the beginning of gliogenesis and later within cortical layers, suggesting an inside-out mechanism by which astrocytes could be distributed within a column[79]. Previous lineage tracing in our lab using the MADM (mosaic analysis with double markers) method found that a similar fraction of clones produce neurons and glia throughout neurogenesis, suggesting that there is no glia-restricted poo of RGPsl.

In addition, we found that a fraction of 1 in 6 RGPs proceed to gliogenesis. Astrocytes and neurons are allocated in radial alignment to restricted domains that can span several layers. This reveals a close spatial association between lineage-related neurons and glia[47].

In summary, as our knowledge of the importance and diversity of glial function increases, it is crucial to bridge the gap of our understanding of the developmental processes that lead to the generation of the proper number and variety of glial cells. Importantly, the relationship between origin and mature heterogeneity of glia is unclear. It is still unknown how astrocyte clones, composed of cells originating from the same progenitor, impact astrocyte heterogeneity and function. A significant hindrance to understanding the developmental basis of glial function and diversity is the lack of markers to selectively target progenitors of these cells types. Here, we carried out analyses of neocortical RGPs that give rise to neurons and glia in order to understand the developmental processes that lead to the diversification of glia at the individual progenitor levels.

Chapter 2

Overview of Experimental Approach for clonal labeling of neocortical radial glial progenitors

2.1 Lineage tracing and clonal analysis of progenitors

Lineage tracing is a developmental biology approach where the origins and fates of tissues are interrogated by labeling single progenitors with an inheritable mark and analyzing their progeny. In clonal analysis, traced progenitors and the resulting clone of daughter cells are studied. This type of analysis reveals how individual progenitors are regulated to ensure the proper structural and functional assembly of tissues. In order to perform clonal analysis of glial progenitors *in vivo*, we took advantage of the MADM (Mosaic Analysis with Double Markers) system[80,81]. We chose MADM as a tracing method as it provides increased information about lineage history of clones. By labeling the two daughter lineages of a progenitor with distinct fluorescent proteins, MADM permits separate tracking of each daughter lineage, increasing our insight into the lineage history of clonally-related cells.

2.2 Lineage Tracing using Mosaic Analysis with Double Markers

MADM is a method adapted from the system MARCM[80], originally developed for the study of genetic mosaics in *Drosophila melanogaster*. Its use for mosaic analysis is based on its ability to uniquely label homozygous mutant cells in an otherwise heterozygous background. MADM relies on two chimeric constructs composed of reciprocal halves of functional fluorescent proteins separated by a loxP site. These constructs are knocked-in to homologous sites on sister chromatids **(Figure 2.1A)**. One MADM allele contains the N-terminus of GFP separated by a loxP site from the the C-terminus of RFP (we refer to this allele as GT). The other MADM allele contains the N-terminus of RFP with the C-terminus of GFP separated by a loxP site (hereafter referred to as TG). After DNA replication in animals heterozygous for the GT and TG alleles, Cre-recombinase, supplied as a separate transgene, mediates inter-chromosomal recombination restoring two functional fluorescent protein cassettes. Upon mitosis, different routes of chromosomal segregation yield two different outcomes in daughter cell labeling: 1) In G_2-X segregation, chromatids encoding fluorescent proteins are segregated into different daughter cells. This results in a daughter lineage permanently labeled red and the other lineage permanently labeled green. 2) In G_2-Z segregation, both chromatids encoding functional fluorescent proteins are segregated to the same daughter cell, while the other daughter cell inherits the two non-functional alleles. This

results in a daughter lineage permanently labeled yellow and while other daughter lineage remains unlabeled. It is also possible for interchromosomal recombination to occur in post-mitotic cells at G0 or G1, which results in an individual cell labeled yellow. In 2010, a version of MADM was made available where GT/TG alleles where knocked-in to the Hip11 locus of chromosome 11 and original MADM RFP, dsRed2, was replaced by tdTomato[82].

Through the supply of a cell type-specific, inducible Cre recombinase, MADM allows clonal analysis in a temporal- and cell type-specific fashion. We take advantage of these properties to perform clonal analysis of neocortical radial glial progenitors (RGPs) which give rise to the neural cell types of the neocortex, namely, neurons, astrocytes, and oligodendrocytes.

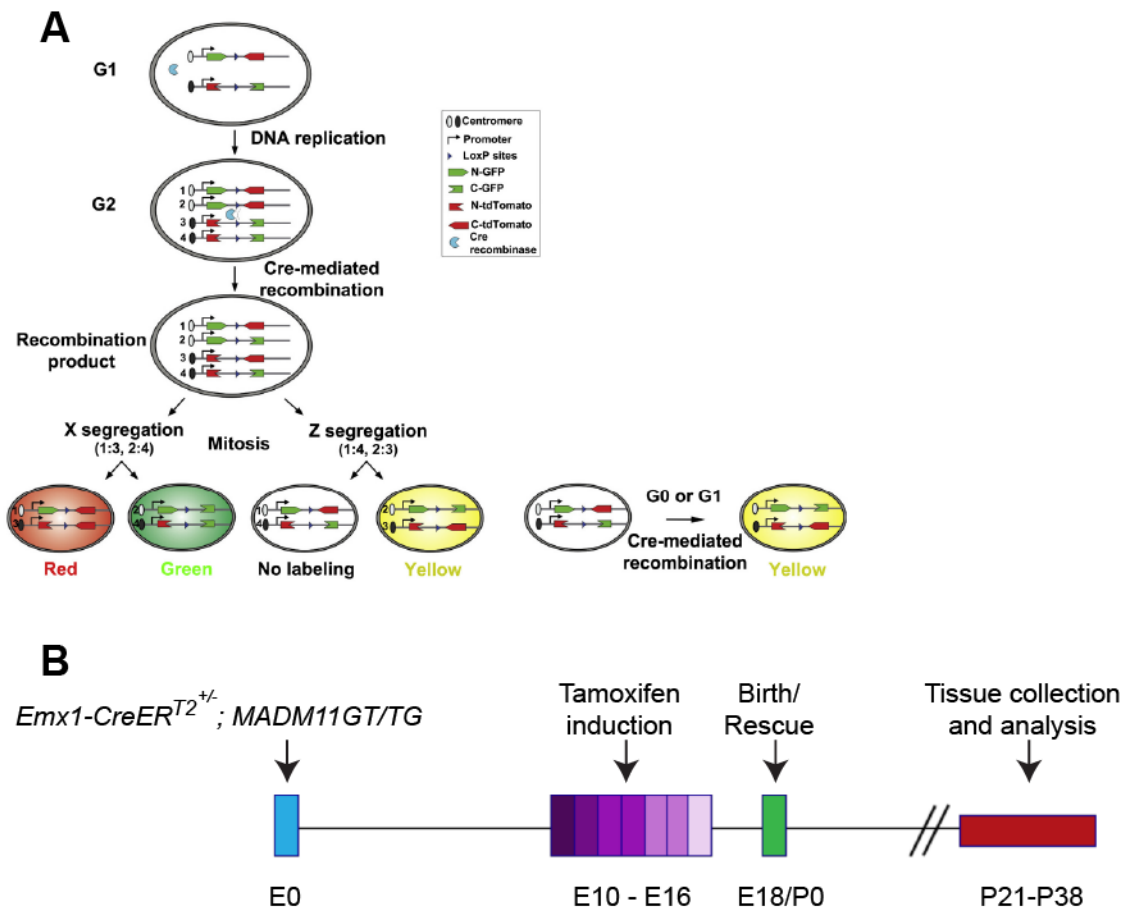

Figure 2.1 Schematic of MADM-based labeling of daughter lineages of dividing progenitors. (A) Heterozygous alleles of MADM replicate in S-phase and are subject to Cre-mediated recombination, restoring functional fluorescent protein cassettes in two chromatids of the dividing progenitors. Allocation of alleles during mitosis results in singly or doubly-labeled daughter lineages. G0 or G1 recombination may restore two fluorescent proteins in a single cell. Figure adapted from Gao *et al. Cell,* 2014[47]. **(B)** Experimental paradigm of MADM-based clonal analysis. A single dose of TM is administered to pregnant females at E10, E11, E12, E13, E14, E15, or E16 and brains are analyzed at P21-P38, when cortical development is largely complete. E, embryonic day; P, postnatal day.

2.3 Approach to clonal analysis of neocortical gliogenesis

The study of glial development has been obstructed by the lack of markers specific to glial progenitors. We circumvent this problem through the tracing of glial lineages derived from a specific subset of the glial progenitors in the forebrain, namely the RGPs of the dorsal telecephalon. In previous MADM-based clonal analysis performed in our lab, we recovered clones of neurons accompanied by glia derived from individual RGPs. By selectively targeting RGPs during late embryogenesis, we are to capture RGPs at their entry into gliogenesis and can use the recovered data to examine the relationships of clonally-related neurons, astrocytes, and oligodendrocytes. We target dorsal RGPs by supplying a CreER^{T2}-recombinase driven by the *Emx1* promoter as a separate transgene. *Emx1* is a transcription factor selectively expressed in dorsal progenitors. With Cre-ER^{T2}, Cre is fused to the extracellular domain of the estrogen receptor. Upon availability of tamoxifen (TM), the ER domain releases the Cre which then is able to translocate to the nucleus and recognize the loxP sites. This allows cell-type and temporal specificity of Cre-mediated recombination.

We administer TM via oral gavage or intraperitoneal injections to timed pregnant damns. We rescued the pups via C-section at E18/P0. We analyzed the brains of adult animals at P21-P38, when cortical development and astrogliogenesis are largely

concluded **(Figure 2.1B)**. Tissue was serially sectioned into 70-100 μm sections. 100 μm sections resulted in us capturing more complete morphologies of cells in individual sections compared to 70 μm sections. We enhanced the intrinsic signal of the expressed GFP and RFP via immunohistochemistry, using antibodies specific to each fluorescent protein. The sections were mounted onto slides for analysis. Full brain scans were performed by either optical detection in an epifluorescent microscope or by scanning entire brains using a slide scanner. Once a clone with mixed green-red cells was identified, we traced the contours of either the entire mounted brain or selected sections corresponding to the clone and its flanking sections, with the software Neurolucida. We labeled positions of cell bodies and drew interlaminar borders based on DAPI signal. Information was recorded about cell identity, cell color, cell position, and neocortical region (**Figure 2.2**). To identify neocortical regions, we used landmarks such as the lateral ventricles and the hippocampus to match our contoured sections to annotated coronal sections of the adult mouse in the Allen Brain Atlas. For instance, the border between the motor cortex and the somatosensory cortex can be identified by finding the lateral border of layer 4.

To recognize a group of cells as belonging to a clone, we used the criteria of isolation and clustering. A clone is identified as a clustered group of labeled cells

separate from any other labeled cells in the brain. In clonal analysis, it is crucial to minimize splitting or lumping errors in identifying clones, which may result from using spatial criteria to identify a clone. Splitting errors result in a single clone of cells identified as multiple clones due to spatial separation of lineage-related cells. Lumping errors result in non-clonally related cells detected as belonging to the same clone due to their proximity. Due to the small size of the clones we analyzed and because glia can undergo extensive migration (eg. OPCs derived from ventral progenitors domains migrate to populate the neocortex, see section 1.5), we want to minimize errors in clone detection. For these reasons, it was crucial we adjust the MADM labeling efficiency to limit the number of clones labeled in individual brains. Sparse labeling is intrinsic to the MADM system, as it requires interchromosomal recombination, a rare event[80]. To further limit the number of labeled progenitors per brain, we titrated our TM dosage until only a few clones were available in each brain. The low dose resulted in very sparse labeling, with several brains per litter devoid of MADM labeling, and others devoid of G_2-X neuron/glia clones. For our brains analyzed at late embryonic inductions the average was 2.4 clones per brain for 38 brains. This averages to 1.2 clones per hemisphere, not including unlabeled brains **(Figure 2.3)**. The efficiency of our labeling allows us to confidently identify clones in our MADM-labeled brains.

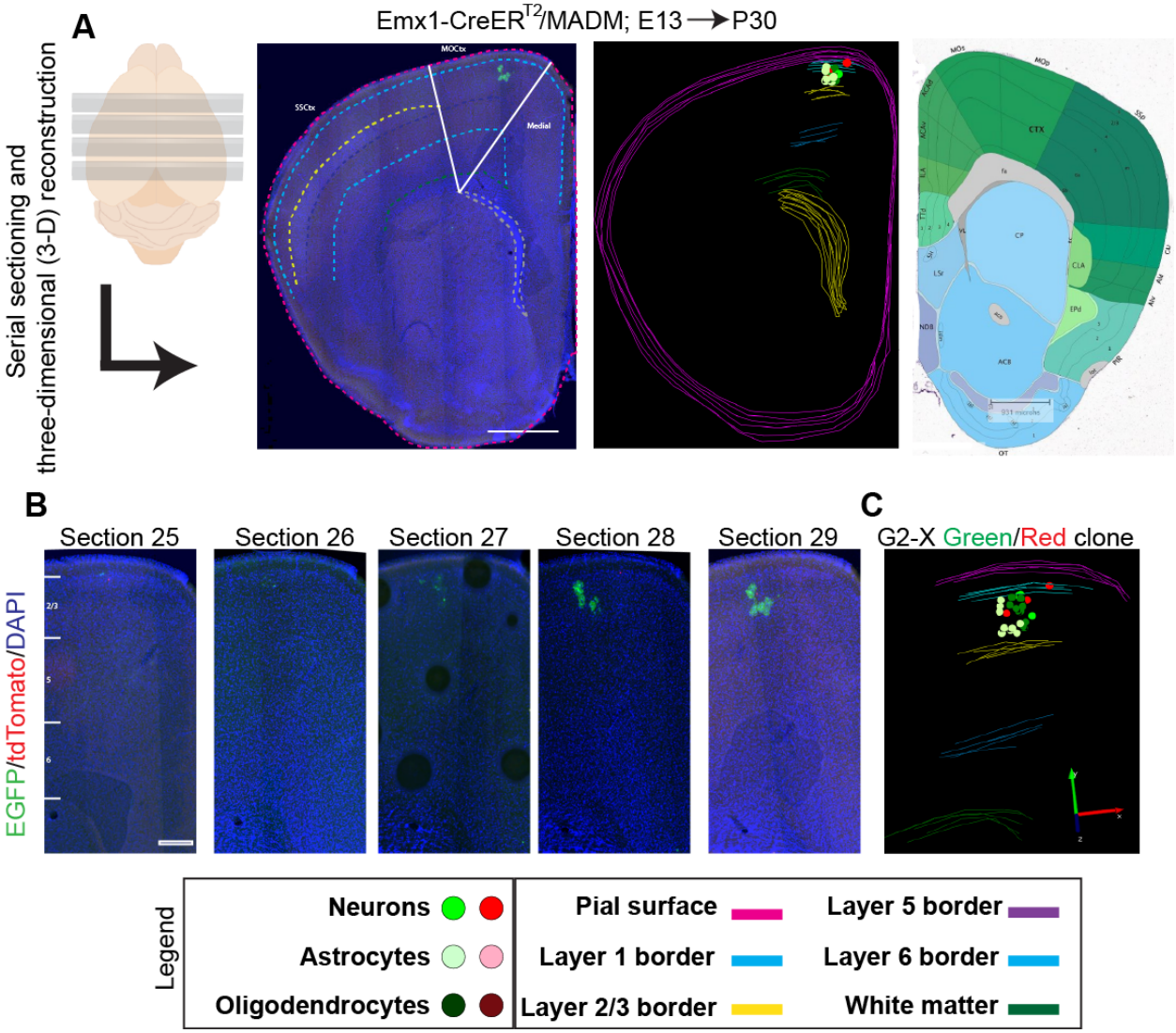

Figure 2.2 Overview of experimental procedure for MADM-based clonal analysis of neocortical gliogenesis. (A) Following coronal serial sectioning and IHC,individual brain sections are examined for MADM labeled cells and contoured based on DAPI signal. Consecutive sections are aligned based on contours. A single recovered clone is reconstructed. Brain Region is identified by matching the countoured sections to the Allen Brain Atlas. **(B) Confocal images of** consecutive sections of the clone shown in A.**(C)** Reconstructed clone from sections in B. Legend shows markers for cell types and laminae utilized throughout 3D reconstructions in this document. (SSCtx, somatosensory cortex; MOCtx, motor cortex). Scale bar 20 μm

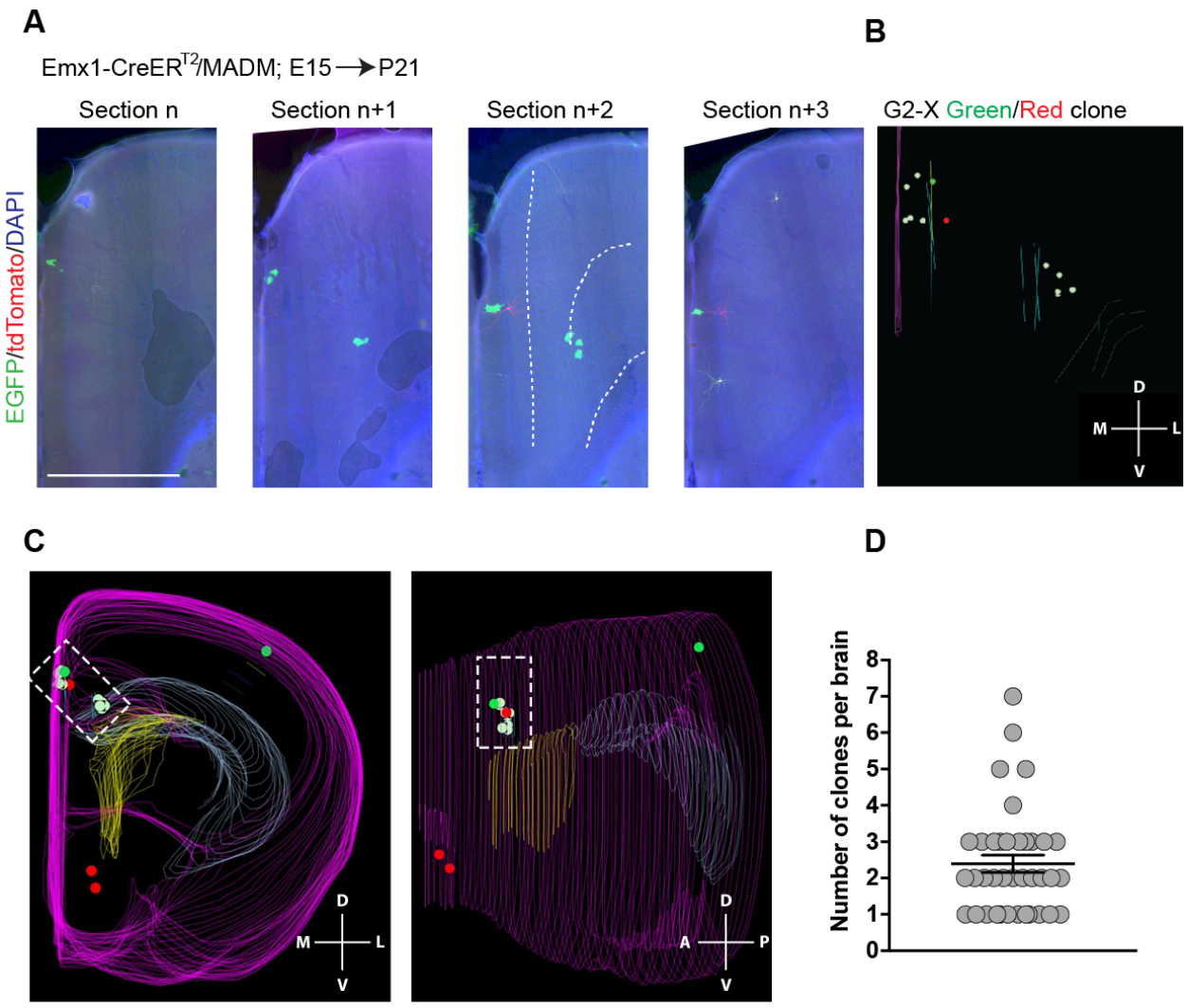

Figure 2.3 Identification of clones using the MADM strategy. Example reconstructed brain and clone using MADM approach. **(A)** Shows confocal microscope images of a G_2-X clone composed of neurons and glia that spans multiple consecutive sections. **(B)** 3D-reconstruction of clone in A. **(C)** Reconstructed MADM labeled brain with all green and red cells marked. An isolated cluster of clonally-related cells selected in dotted box. Large yellow structure corresponds to left lateral ventricle. Large blue structure represents outline of hippocampal layers. **(D)** Quantification of number of labeled of G_2-X MADM gliogenic clones per brain at late inductions E13-E16. (n = 38 brains, data presented as individual points per clone, bars indicate mean ± SEM. D, dorsal; V, ventral; M, medial; L, lateral; A, anterior; P, posterior.

2.4 Identification of glial subtypes by molecular and morphological criteria

Astrocytes and oligodendrocytes in the neocortex are readily distinguished by their characteristic morphologies, as validated by using established markers for these cell types **(Figure 2.4, Figure 2.5)**. Molecularly, astrocytes are characterized by the expression of the intermediary filament protein GFAP (glial fibrillary acidic protein). The three recognized astrocytic subtypes differ in their characteristic morphologies. Protoplasmic astrocytes, which are found throughout the gray matter are characterized by a "bushy morphology". They have 4-6 thick main branches that extend radially from the soma and the continue to branch off into gradually finer processes that occupy a large fraction of the volume that surrounds the cell body. Fibroblast-like astrocytes are found adjacent to the pia mater. Instead of radial processes, this astrocyte subtype has a flat structure that runs parallel to the pia matter **(Figure 2.4, B'')**. Fibrous astrocytes in the white matter, similar to protoplasmic astrocytes, exhibit several thick main branches that extend radially from the cell body accompanied by finer, but still relatively thick branches. We confirmed that these cells are in fact astrocytes by co-staining with GFAP **(Figure 2.4)**.

Oligodendrocyte subtypes exhibit a range of morphologies and molecular profiles that reflect the various intermediate stages towards their functional

differentiation from OPCs to fully differentiated myelinating oligodendrocytes. OPCs are characterized by a "lacy" morphology with several thin processes that extend radially from the soma. OPC radial processes differ from those of protoplasmic astrocytes because they do not occupy a large fraction of their surrounding volume, so they lack the "bushy" appearance. OPCs also lack the thick main branches characteristic of astrocytes. Another feature that distinguishes oligodendrocytes from astrocytes is the relatively smaller soma. OPCs are positive for the transcription factor Olig2 (oligodendrocyte transcription factor) (**Figure 2.5 D, D').** Immature oligodendrocytes combine features of OPCs and mature oligodendrocytes. The immature oligodendrocyte population is composed by several intermediate oligodendroglia subtypes that have committed to differentiation[40]. They have a combination of the fine radial processes of OPCs, and the thin processes that extend parallel to axonal tracts of myelinating oligodendrocytes. These cells are also positive for the transcription factor *Olig2*. Myelinating oligodendrocytes are more frequently found in the white matter and have processes that run parallel to axonal tracts.

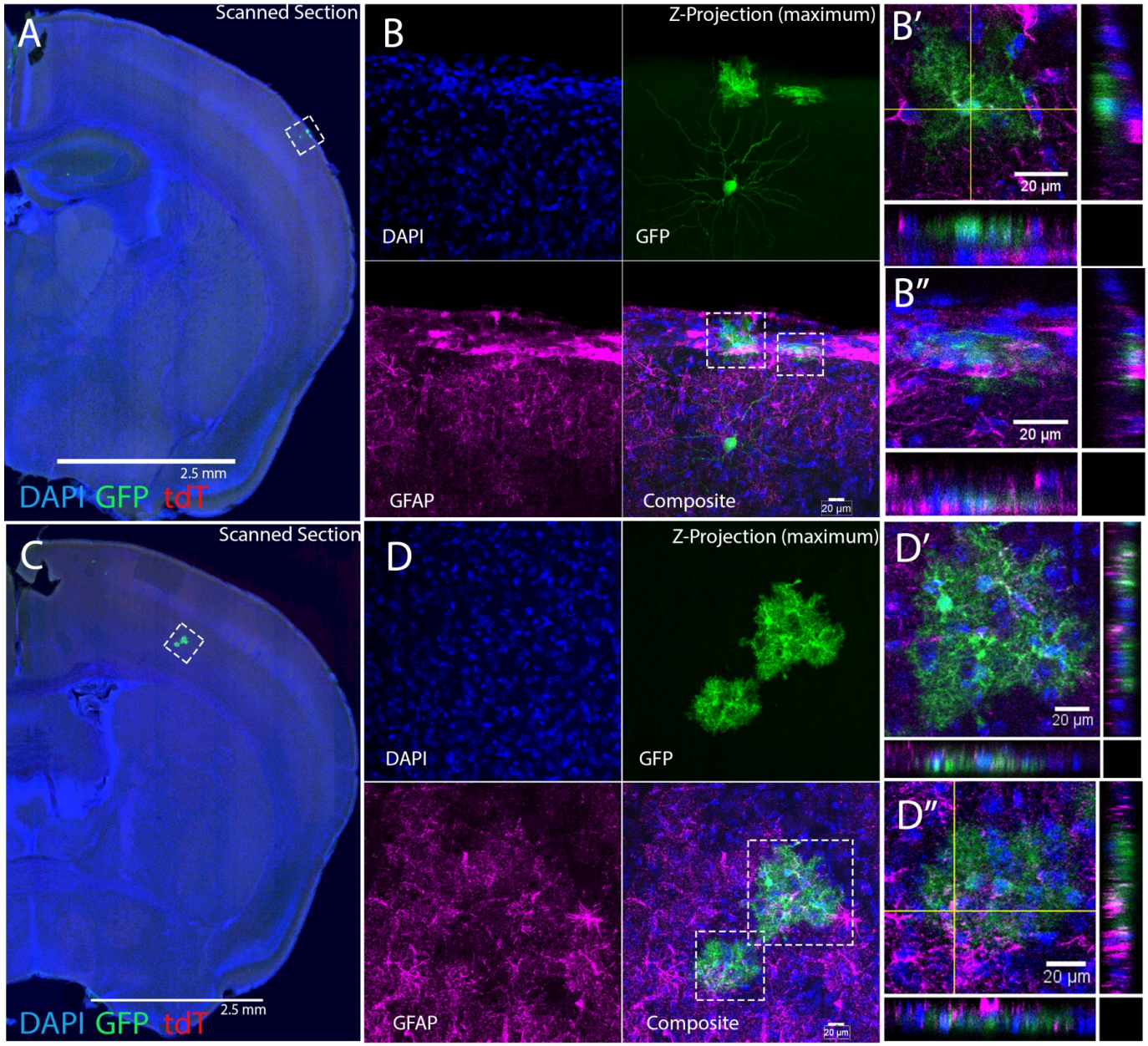

Figure 2.4 Identification of *Emx1*-MADM labeled astrocytes. (A) and **(C)** show non-consecutive sections in the same brain, cells belong to two separate clones. **(B)** and **(D)** are Z-projections of 20X confocal images of cells selected in A and C, respectively. **(B′,B″)** and **(D′,D″)** show Z-projections of 60X confocal images of the areas selected in B and D, respectively. XZ and YZ planes are shown along the axes.

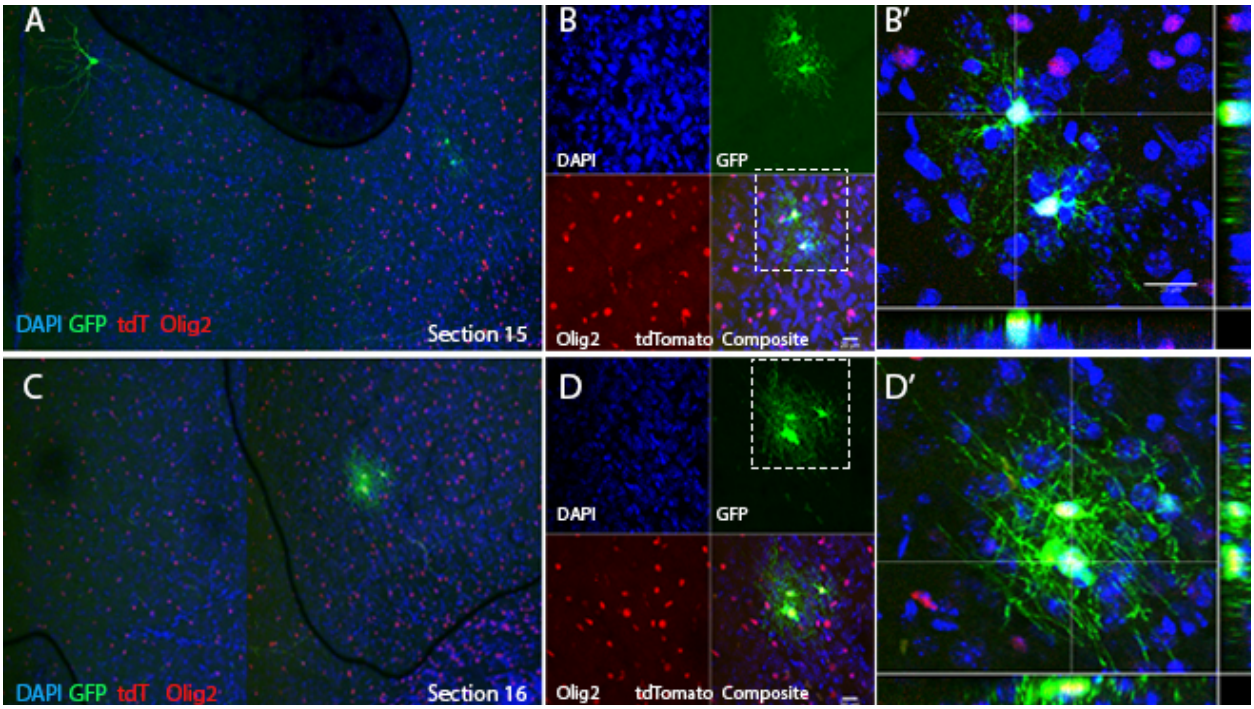

Figure 2.5 Identification of *Emx1*-MADM labeled oligodendrocytes. (A) and **(C)** are consecutive sections with oligodendrocytes belonging to the same clone. Images are Z-projections of 10X confocal images. **(B)** and **(D)** Are Z-projections of 20X confocal images of cells in A and C, respectively. **(B′)** and **(D′)** show 60X Z projections of the areas selected in B and D, respectively. XZ and YZ planes are shown along the axes. Scale bar, 20 μ

2.5 Comparison of TM-mediated Cre-ER recombination via different administration routes

In order to capture the final neurogenic divisions and entry into gliogenesis of RGPs, we performed TM induction at late embryonic stages E14, E15, and E16. At the earlier induction time points E10, E11, E12, and E13, TM was administered via intraperitoneal (IP) injection to pregnant dams. The maximum dose used at E10-E13 was 50 μg/g body weight. However, when we attempted administer this dose via IP injection to dams at E14-E16, it resulted in miscarriages and embryo malformations that led to perinatal death (P0-P4). For this reason, we performed TM administration via oral gavage which led to increased embryo survival. This may be due to difference in the metabolism of TM that enters through the peritoneum or the gastrointestinal tract. With progression of embryonic time, TM dosages need to be increased in order to induce recombination in dividing progenitors. We believe this is due not only to an increase in embryo size, but also a reduced availability of dividing progenitors as they exit cell cycle. For E14-E16 inductions, the dosage was adjusted to a dose of 200-250 μg/g body weight via oral gavage.

We were concerned that different methods of TM administration may affect the onset of Cre-ER mediated recombination due to differences in metabolism between the different routes used. This may affect the window during which RGPs are labeled resulting in a temporal gap that may confound the comparison of data obtained from consecutive time points via different administration routes. If there is a significant difference in time of recombination by IP and oral gavage, we would expect a significant difference in clone sizes obtained through each method at the same time point. This difference would correspond to progenitors labeled earlier or for a more prolonged period via one route relative to the other. We compared clone size, as total number neurons per clone and as total glia per clone, in G_2-X clones that contained a mixture of neurons and glia at E13 induced by IP administration and oral gavage. We found that administration of TM via different routes does not significantly affect clone size **(Figure 2.6)**. This indicates that TM-mediated induction occurs with a similar delay upon administration by both methods.

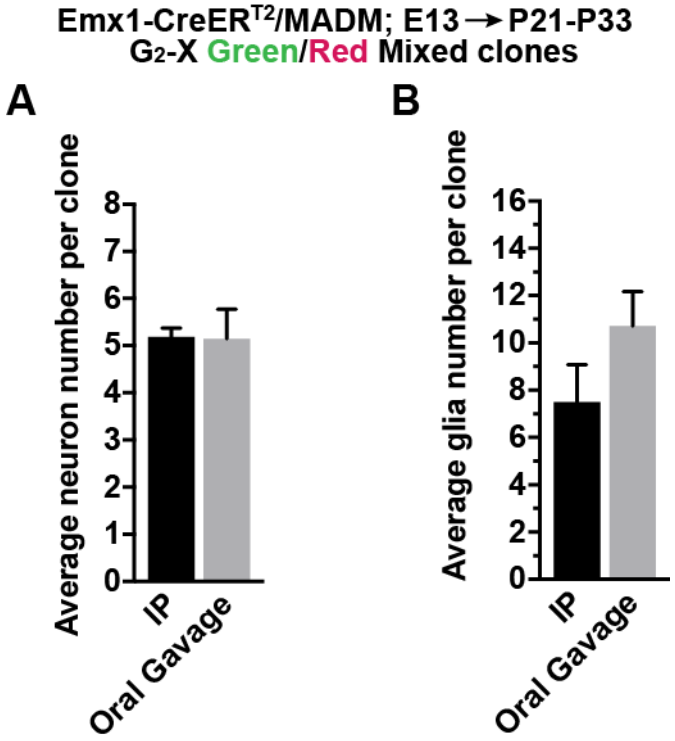

Figure 2.6 Quantification of clone size of *Emx1*-MADM labeled clones composed of a mixture of neurons and glia. (A) Quantification of total neuron number per clone. **(B)** Quantification of total glia number per clone. All inductions were performed at E13. (IP, n = 16; oral gavage, n = 40). Data are presented as mean ± SEM. n.s., not significant.

Chapter 3

Gliogenesis in the neocortex at the individual radial glia progenitor level

3.1 Late embryonic MADM labeled progenitors capture RGP entry into gliogenesis

Previous published work from our lab showed that while a majority of RGPs exit cell cycle at the end of neurogenesis, a defined fraction of 16%, roughly 1 in 6 progenitors, proceeds to gliogenesis. Although we recovered some clones composed of only glia, we focused our analysis of gliogenesis on the subset of clones that contain a mixture of neurons and glia (hereafter referred to as mixed clones). It is established that RGP neurogenesis precedes gliogenesis. Therefore, we expect that mixed clones capture the full gliogenic output of RGPs.

Consistent with the progression of neurogenesis through embryonic development, we found a gradual decrease in neuron number in clones from E10-E16 **(Figure 3.1A)**. This corresponds to the diminishing potential of RGPs transition from

earlier rounds of symmetric division, where the pool of RGPs is expanded, to asymmetric division where they are restricted to produce either Tbr2-positive intermediate precursor cells, neurons, and/or glia. Our lab has established that the output of a single RGP is a "quantum" of 8-9 neurons[83]. Clones labeled at E10 to E12 produce a number of neurons several multiples the size of the neurogenic quantum, corresponding to multiple RGPs in the labeled clone. RGPs labeled at later stages capture fewer of these symmetric divisions, resulting gradually smaller clones until E13, where the majority of clones undergo asymmetric division. This is consistent with our previously published work that finds clonal expansion by symmetric division is predominant at early developmental stages. Clones labeled at E13-E16 contained a clone size of neurons that averages below the unit size, which indicates we are labeling individual RGPs **(Figure 3.1A, B)**. Clone size continues to decrease from E13 to E16 as RGP proliferative capacity is depleted through sequential rounds of division as they produce their final neurons.

Similarly, when we examine the gliogenic output of mixed G_2-X clones, we find that from E10 to E11 there is a significantly larger number of glia labeled in each mixed clone **(Figure 3.1C).** This is consistent with symmetric expansion of RGPs which increases the probability of having more than one gliogenic RGP per clone. However,

we find a comparable number of total glia (astrocytes plus oligodendrocytes) labeled in clones from E13-E16 **(Figure 3.1C, D)**. These stages correspond to asymmetrically dividing clones, where we are labeling an individual RGP. Because our glia number accounts for the combination of astrocytes and oligodendrocytes, we also quantified these glia types separately. We found, consistent with the result for total glia, a constant number of astrocytes and oligodendrocytes produced by progenitors labeled from E13 to E16 **(Figure 3.1E, F)**. These results indicate when we capture the asymmetric neurogenic phase of RGPs, we can capture their full gliogenic output. If this is true, we would predict that there is no correlation between neuronal output and glial output in asymmetric mixed clones. Our analysis revealed no correlation between total number of neurons and total number of glia in clones labeled at E13 to E16 **(Figure 3.1G)**.

Together these results suggest that there is a regulation in the number of glia produced by an individual RGP independent of when exit from neurogenesis occurs. A consistent distribution of clone sizes throughout these final neurogenic stages allows us to combine the data recovered from E13-E16 inductions for further analysis.

One caveat of our method is that the total number of glia identified in our MADM-labeled clones may not be equal to the total number of glia that progenitor

produces: while it has been demonstrated that there is no extensive cell-death in the cortex in the excitatory neuron lineage, there is no conclusive evidence whether there is a postnatal period of glial pruning, where glial cells are removed.

Figure 3.1 Quantification of MADM neuron-glia clone size. (A) Quantification of total neuron number per mixed clone. (P21-P40: E10, n=12; E11, n =13; E12, n = 9; E13, n = 56; E14, n = 30; E15, n =20; E16, n =3). **(B)** Quantification of neuron number per mixed clone, from E13-E16 data shown in A. **(C)** Quantification of total glia number per mixed clone (sum of astrocytes and oligodendrocytes). **(D)** Only shows E13-E16 data in C. **(E)** Quantification of oligodendrocyte number per clone at E13-E15 inductions, for clones which contain oligodendrocytes. (**F)** Quantification of astrocyte number per clone at E13-E15 inductions, for clones which contain astrocytes. **(G)** Scatterplot of the size of clone glia number versus the size of the clone neuron number for individual mixed clones at E13-E16 inductions. A, B, data presented as mean ± SEM. B, D, E, F, points represent individual clones, bars indicate mean ± SEM. (*$p < 0.05$, **$p< 0.01$,***$p < 0.001$, ****$p < 0.0001$)

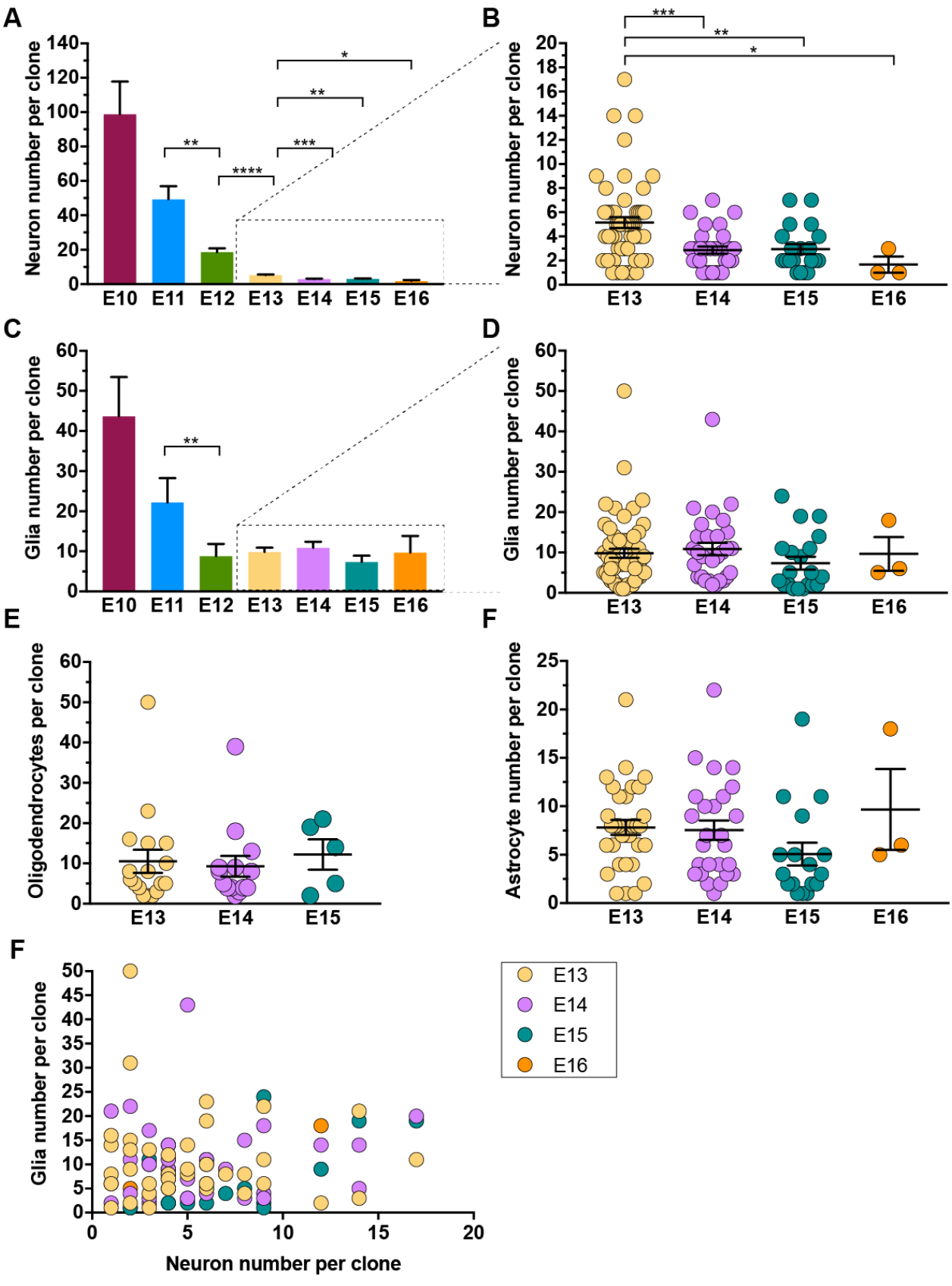
A
Neuron number per clone
E10
E11
E12
E13
E14
E15
E16
B
Neuron number per clone
E13
E14
E15
E16
C
Glia number per clone
D
Glia number per clone
E
Oligodendrocytes per clone
F
Astrocyte number per clone
F
Glia number per clone
Neuron number per clone
E13
E14
E15
E16

3.2 Three different types of gliogenic progenitors differ in their potential to produce glial subtypes

Our analysis at single-RGP resolution uncovered three distinct clone types based on their capacity to make neurons, astrocytes, and/or oligodendrocytes. One type produces neurons and astrocytes, the second type produces neurons and oligodendrocytes and the third type produces neurons, astrocytes, and oligodendrocytes; we will refer to these types as N+A, N+O, and N+A+O, respectively **(Figure 3.2A)**. That we uncovered clones that only have astrocytes or oligodendrocytes and clones that have both glial subtypes indicates that not all progenitors need undergo a sequence of making one glial subtype prior to making the other.

We further wanted to compare tri-potent N+A+O progenitors with their bi-potent N+A and N+O counterparts to examine if there was a difference in proliferative capacity associated with their potential to generate more cell types. Indeed, N+A+O clones produce on average twice as much glia than N+A and N+O progenitors (N+A+O, 16.3 ± 2.0; N+A, 7.5 ± 0.7; N+O, 10.7 ± 3.2). However, when we compare output of individual cell types, we find no significant difference between the number of astrocytes of N+A+O clones and N+A clones (**Figure 3.2C**; N+A+O, 7.5 ± 0.7; N+A, 6.3 ± 0.7), nor in

the number of oligodendrocytes in N+A+O clones compared to N+O (**Figure 3.2D**; N+A+O, 10.0 ± 2.0; N+O 10.7 ± 3.2).

Examination of individual N+A+O clones showed no correlation between the astrocyte and oligodendrocyte output. Together these data suggest that the determined output of glia for NA+O, N+A, and N+O gliogenic RGPs is not the same amount. If there were a similar output for all gliogenic RGPs, in N+A+O clones making more than one subtype would result in a decreased output of the other; but we observe an overall increase in the number of glia produced in N+A+O RGPs compared to their N+A and N+O counterparts **(Figure 3.2E)**. This also suggests that oligodendrocyte and astrocyte precursors that arise from a common RGP maintain their intrinsic proliferative potential.

3.3 Distribution of RGP subtypes is similar across late embryonic time points and neocortical brain regions

To examine whether there is a temporal gradient in specification of RGP subtypes, we examined the proportions of each mixed clone type in clones recovered from E13 to E15 inductions. We focused on these time points as they are our most sampled late embryonic time points. If a temporal gradient in RGP subtype specification exists, we would predict a shift in the proportion of different clone types,

with a gradual decrease of earlier-specified types and a concomitant increase in later-specified clone types. Our data does not reveal a significant difference in the proportion of clone types across different induction time points. This suggests that a constant proportion of different clone types are specified from the same pool of progenitors, independent of the time they enter gliogenesis. The proportion and output of different RGP types are consistent throughout neocortical brain regions **(Figure 3.3B).** Together these data suggest that proportions of different progenitor types and their gliogenic capacity are a general property independent of cortical region. This is similar to our previously published data that shows that neurogenic output of clones is also similar across cortical regions[83].

Figure 3.2 Three different mixed RGP subtypes based on their composition have distinct proliferative potential. (A) Shows 3D reconstructions of consecutive sections that contain MADM labeled clones with distinct potential: RGPs that generate neurons (solid color), astrocytes (light shades), and oligodendrocytes (dark shades), N+A+O; clones that generate neurons and oligodendrocytes, N+O, and clones that generate neurons and astrocytes, N+A. Laminar borders determined by DAPI staining are depicted as lines. **(B)** Quantification of total glia number per clone. **(C)** Quantification of astrocyte number per clone in N+A+O and N+A clones. **(D)** Quantification of oligodendrocyte number per clone in N+A+O and N+O clones. **(E)** Scatterplot of oligodendrocyte number versus astrocyte number per clone for N+A+O clones. Clones induced E13-E16; analyzed P21-P40: N+A+O, n = 21; N+A, n = 57; N+O, n = 15). B-D Individual clone sizes shown as points, bars show mean ± SEM. **p < 0.01; **** p < 0.0001; n.s., not significant.

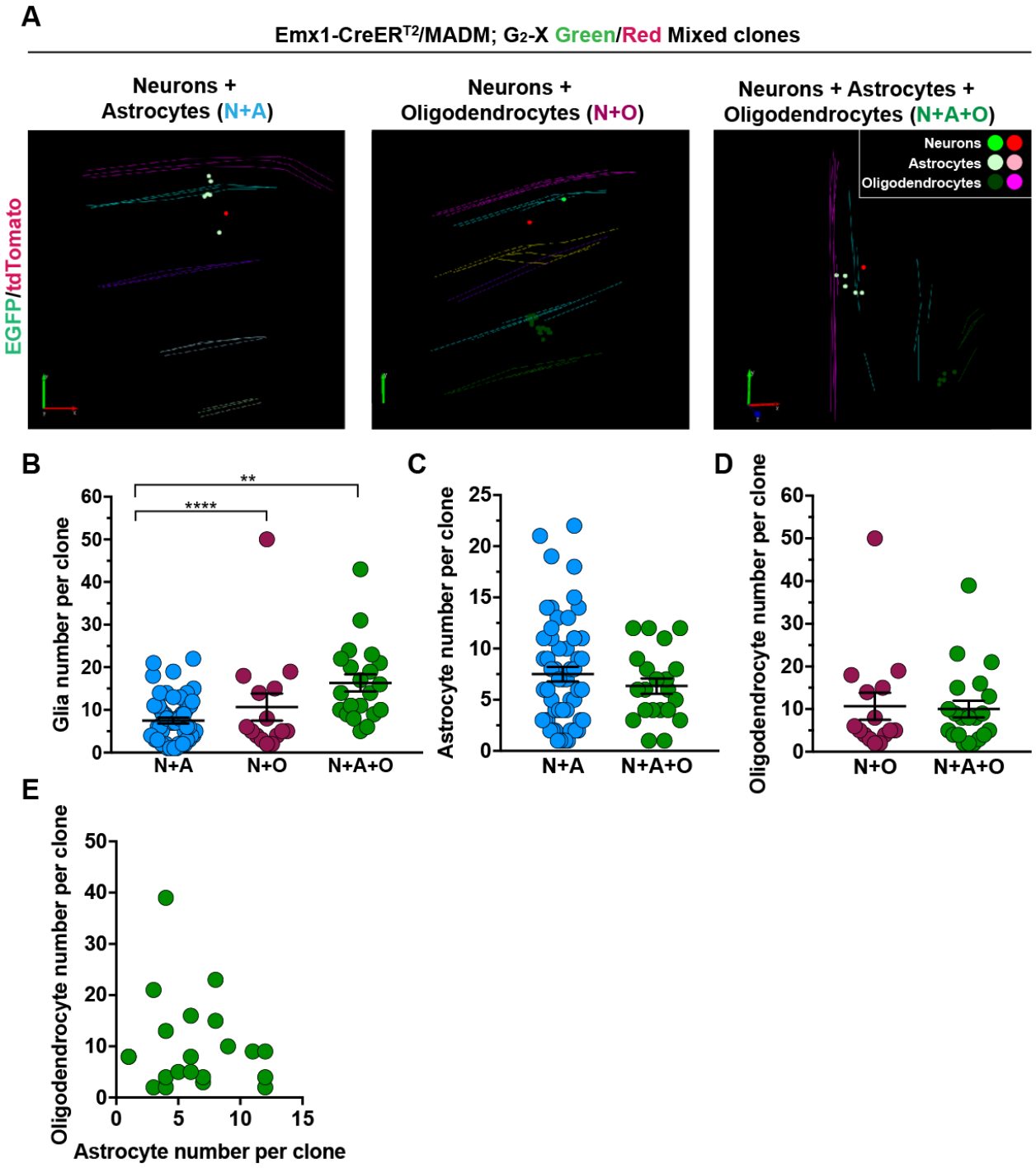
A
Emx1-CreER^{T2}/MADM; G$_2$-X Green/Red Mixed clones
Neurons + Astrocytes (N+A)
Neurons + Oligodendrocytes (N+O)
Neurons + Astrocytes + Oligodendrocytes (N+A+O)
EGFP/tdTomato
Neurons
Astrocytes
Oligodendrocytes
B
Glia number per clone
**
****
N+A
N+O
N+A+O
C
Astrocyte number per clone
N+A
N+A+O
D
Oligodendrocyte number per clone
N+O
N+A+O
E
Oligodendrocyte number per clone
Astrocyte number per clone

Figure 3.3 RGP subtype distribution is similar across developmental time points and brain regions. **(A)** Percentage at N+A+O, N+A, and N+O mixed clones at E13, E14, E15 inductions. **(B)** Percentage of different RGP types located in different neocortical areas. **(C)** Quantification of glial output of clones in different neocortical areas. (Medial, n = 12; MO, n = 18; SS, n = 22). **(D)** Quantification of astrocytes production in clones in different neocortical areas. (Medial, n = 9; MO, n = 13; SS, n =19) **(E)** Quantification of oligodendrocyte number of clones located in different neocortical areas. (Medial, n = 6; MO, n = 6; SS, n = 8). SS, somatosensory cortex; MO, motor cortex; RSP, retrosplenial area; PTLp, posterior parietal association areas; VISal, visual cortex; AUD, auditory cortex; Medial includes: anterior cingulate area, infralimbic area, and prelimbic area.

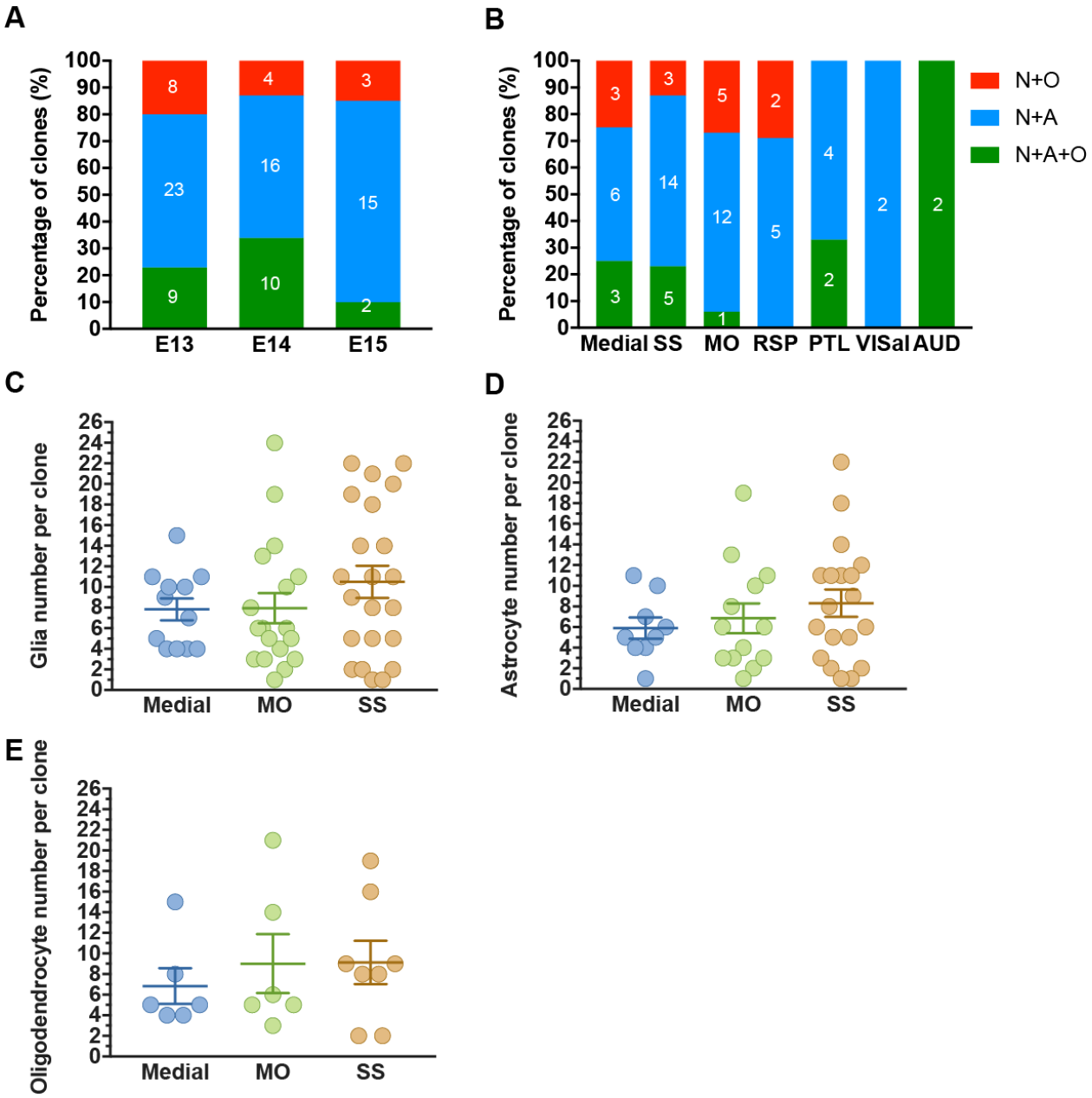
A
Percentage of clones (%)
E13
E14
E15
B
Percentage of clones (%)
Medial
SS
MO
RSP
PTL
VISal
AUD
N+O
N+A
N+A+O
C
Glia number per clone
Medial
MO
SS
D
Astrocyte number per clone
Medial
MO
SS
E
Oligodendrocyte number per clone
Medial
MO
SS

3.4 Analysis of clone transitioning into gliogenesis uncovers different dynamics for RGP exit from neurogenesis

To further dissect the dynamics through which glia are specified from a single progenitor, we decided to focus on the cases where we recovered putative clones at the exit from neurogenesis We defined these as clones that have a single neuron accompanied by glia. Comparison of the fraction of single-neuron clones at different time points shows that a similar proportion of clones transition out of neurogenesis across the analyzed embryonic stages. This suggests a fixed rate at which RGPs, which represent a temporally uncoordinated population, exit neurogenesis and transition into gliogenesis through asymmetric division stages **(Figure 3.4A)**. Most of the clones (57.9%) were composed of one daughter lineage composed of one neuron and the second daughter lineage composed purely of glia. This is the expected outcome for progenitors that proceed to produce glia after their final neurogenic division. However, we also uncovered two other cases of single neuron clones that do not correspond to a transition into gliogenesis. (1) clones where the neuron and the accompanying glia are all labeled in the same color (31.6%). These clones very likely arise from the first division where the daughter lineages are labeled, the daughter RGP in one lineage continues neurogenesis and proceeds to gliogenesis, while the labeled cell of the second lineage undergoes cell death. Recent studies indicate that there is reduction in the

number of neocortical excitatory neurons between P2 and P5, with the population dropping approximately 12% between these postnatal development stages, and then remaining stable into adulthood.[84] (2) In a fraction of the cases, 10.5%, the neuron is labeled one color and the glia are labeled in both colors. It is likely this clone is the result of an initial division whereby the daughter lineages are labeled. One lineage specifies a glia-restricted precursor; while the RGP in the second daughter lineage self-renews, produces the final neuron from neurogenesis, then proceeds to gliogenesis. This result suggests that gliogenesis may occur concurrently with neurogenesis from the same parent RGP. That is, the glia lineage of a progenitor may be produced while it is still in the neurogenic phase. This data differs from the established sequence of neurogenesis preceding gliogenesis.

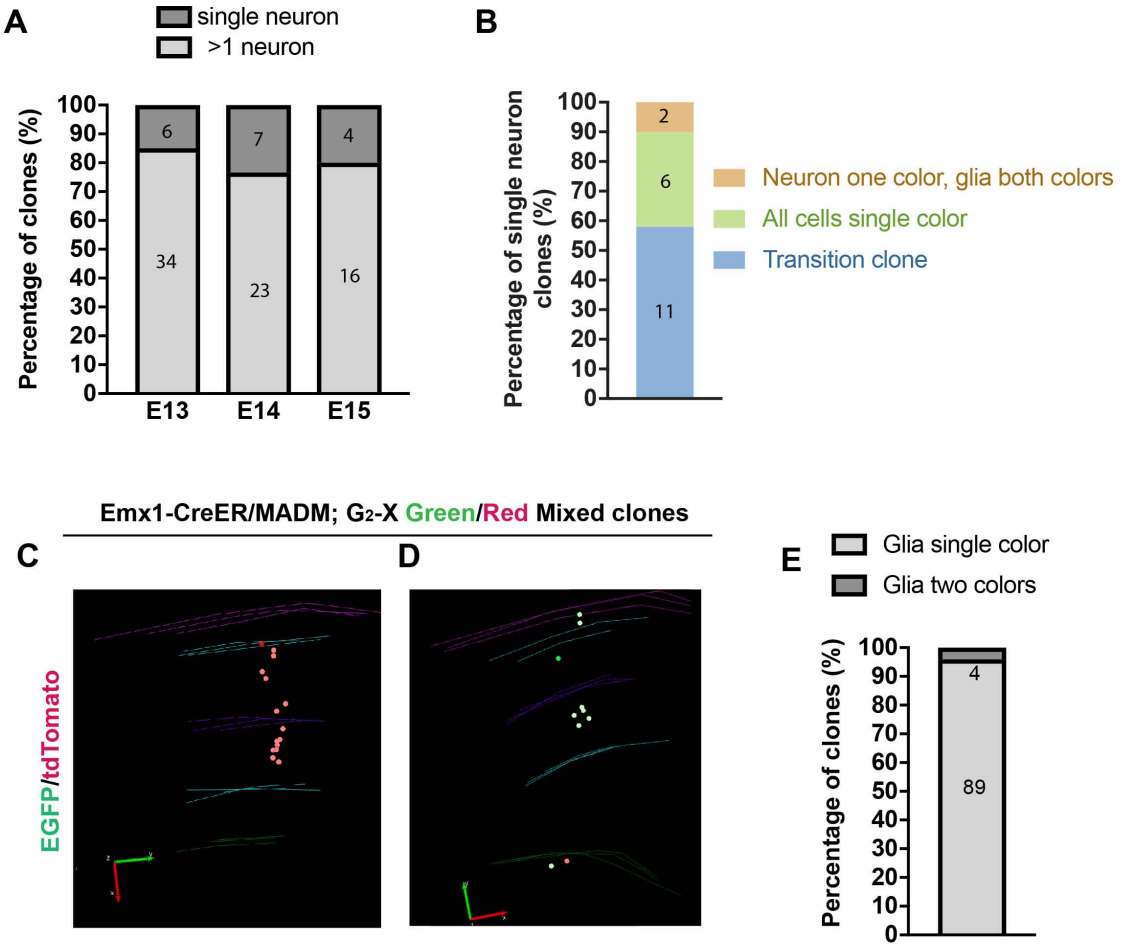

Figure 3.4 Quantitative analysis of mixed clones transitioning from neurogenesis to gliogenesis reveals RGP behavior. (A) Percentage of single neuron clones recovered from E13 to E15 inductions. **(B)** Percentage of single neuron clones by composition and color of neuron and glia lineages. **(C)** Percentage of all G_2-X mixed clones by color composition of their glia. **(D)** 3D reconstruction of a mixed single color clone. **(E)** 3D reconstruction of a mixed clone with glia in two colors.

3.5 Different dynamics underlie proliferation of astrocytes and oligodendrocytes

The frequency distributions of clone sizes for astrocytes and oligodendrocytes differ. About 10% of clones with astrocytes produce only 1 astrocyte. However, all clones containing oligodendrocytes produced ≥2 oligodendrocytes. This result is similar between N+A+O clones and their bi-potent counterparts **(Figure 3.5, A, B)**, which suggests different mechanisms regulate the number of astrocytes and oligodendrocytes produced by individual RGPs. This finding further supports that astrocyte- and oligodendrocyte-restricted precursors derived from RGPs maintain their intrinsic properties when they are derived from a common (NAO) progenitor.

Although our sampling is inconclusive, the dataset suggests a difference in distribution of astrocyte and oligodendrocyte clone sizes. When we examine the frequency distribution of different clone sizes, we find similar frequencies of clone sizes from 1-14 astrocytes, with a much smaller probability for larger clones. For oligodendrocytes, there seems to be a bimodal distribution, with one curve describing the probabilities of smaller clones 1-8 and another curve describing larger clone sizes 13-24 **(Figure 3.5C, D)**. Because the distribution of glia clone sizes are not randomly dispersed, but seems to be centered at different peaks, this suggests that gliogenesis is

not a stochastic event but that there is a constraint in the glial output of individual progenitors.

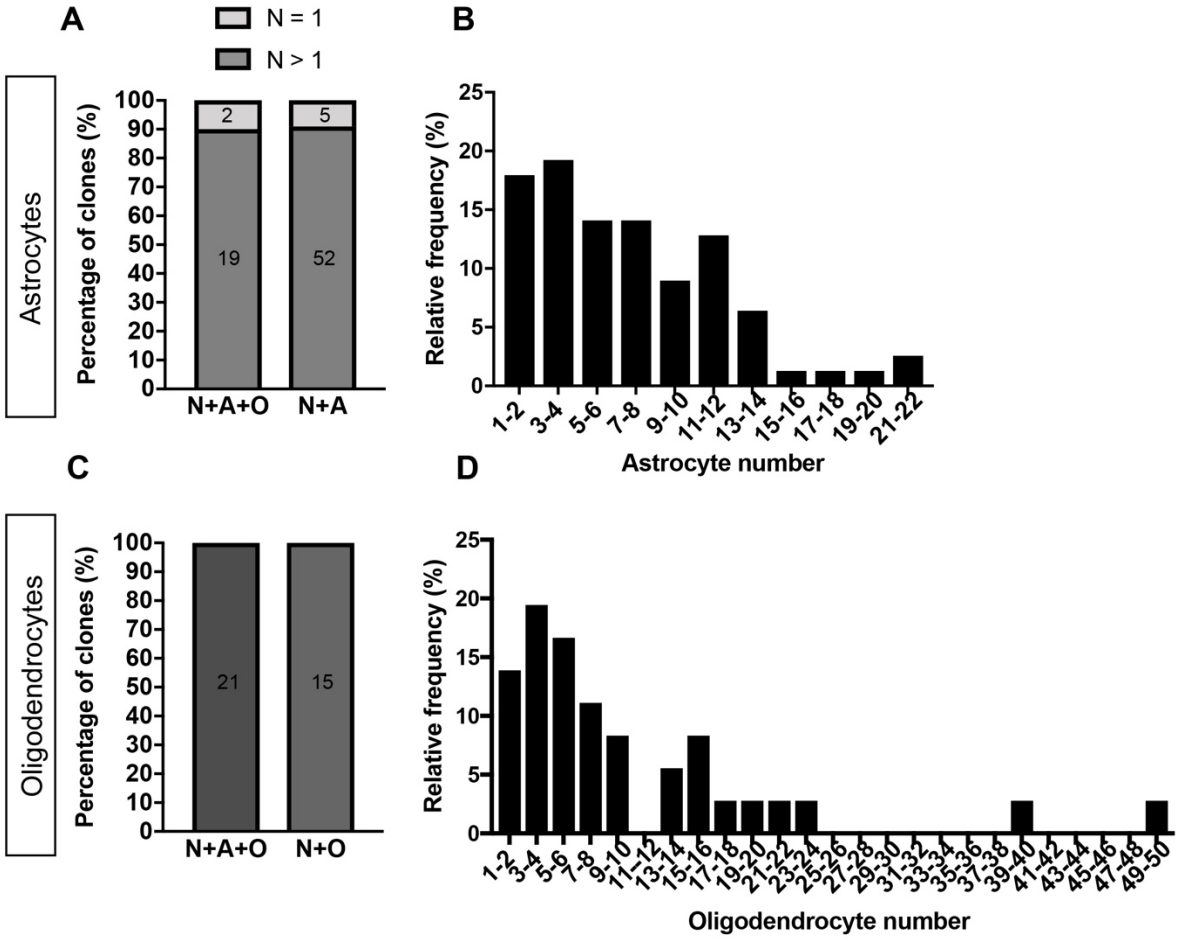

Figure 3.5 Quantitative analysis of astrogliogenesis and oligodendrogenesis. (A) Percentage of clones composed of a single astrocyte or n>1 astrocyte, by clone subtype. **(B)** Percentage of clones composed of a single oligodendrocyte or n>1 oligodendrocytes, by clone subtype. **(C)** Histogram of frequency distribution of clone sizes by astrocyte number. **(D)** Histogram of frequency distribution of clone sizes by oligodendrocyte number

3.6. Contrast in the distribution of RGP-derived astrocytes and oligodendrocytes

The following sections focus on the distribution of glia in a clone. In the neocortex, excitatory neuron cytoarchitecture reflects function, whereby neurons distributed through different lamina have differing properties but are similar to those within their layer, as explained in section 1.3. Astrocyte subtypes are partially distinguished by location, so lamina can be used as a proxy to gain insight on how subtype heterogeneity is established for neocortical glia.

Most oligodendrocyte clones (77.8%) are clustered into a single layer **(Figure 3D**). These single layer clones are mostly found in layer 4 **(Figure 3E)**. This is compared to astrocytes, where a smaller fraction (36%), are restricted to a single layer **(Figure 3B)**. Astrocytes clones that span a single layer are mostly found in the white matter **(Figure 3C)**. Because white matter astrocytes are of the fibrous subtype, this result suggest that fibrous astrocytes have a diminished migratory and/or proliferative capacity compared to protoplasmic and 'fibroblast-like' astrocytes. We cannot conclude whether this is a property intrinsic of the cell type, or whether the WM is a less permissive environment for astrocyte proliferation compared to GM.

For clones where glia spans multiple layers, we see a wider spread in the distribution of astrocytes compared to that of oligodendrocytes **(Figure 3.7 A, C)**. Oligodendrocyte clones are mostly distributed in deep cortical layers. If the clone is spread throughout multiple layers, it is mostly adjacent layers between Layer 5 and the white matter. If we examine the total oligodendrocyte population recovered by MADM clonal labeling, we also find that most oligodendrocytes are destined for deep cortical layers (layers 5-6) and the white matter, with 59.2% and 18.5% of oligodendrocytes, respectively **(Figure 3.7 D)**. A smaller fraction, 9.3% of oligodendrocytes are destined for the superficial cortical layers 2-4, and only 3.1% of oligodendrocytes are destined for pia-Layer 1. This contrasts with the distribution of astrocytes where 41.1% of total recovered astrocytes are destined for layers spanning the pial surface to layer 4.

Figure 3.6 Laminar locations of clones that span a single cortical layer. (A) 3D reconstrcuted clones show representative cellular distributions in different clone types. **(B)** Fraction of mixed clones where astrocytes are restricted to one layer. **(C)** Laminar location of single-layer astrocytes. **(C)** Fraction of mixed clones where oligodendrocytes are restricted to one layer. **(D)** Laminar location of single-layer oligodendrocytes.

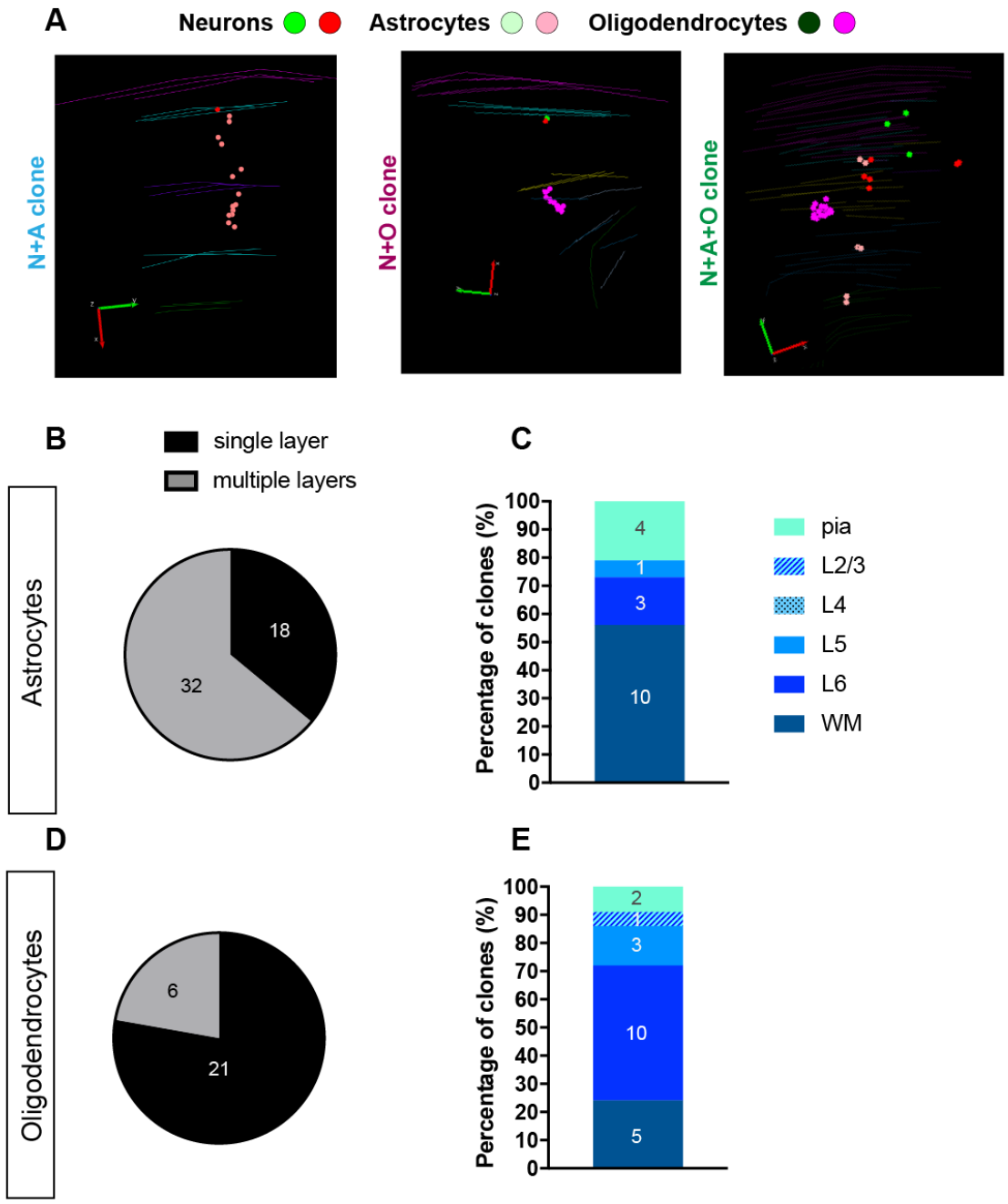
A
Neurons
Astrocytes
Oligodendrocytes
N+A clone
N+O clone
N+A+O clone
B
single layer
multiple layers
Astrocytes
18
32
C
Percentage of clones (%)
4
1
3
10
pia
L2/3
L4
L5
L6
WM
D
Oligodendrocytes
6
21
E
Percentage of clones (%)
2
1
3
10
5

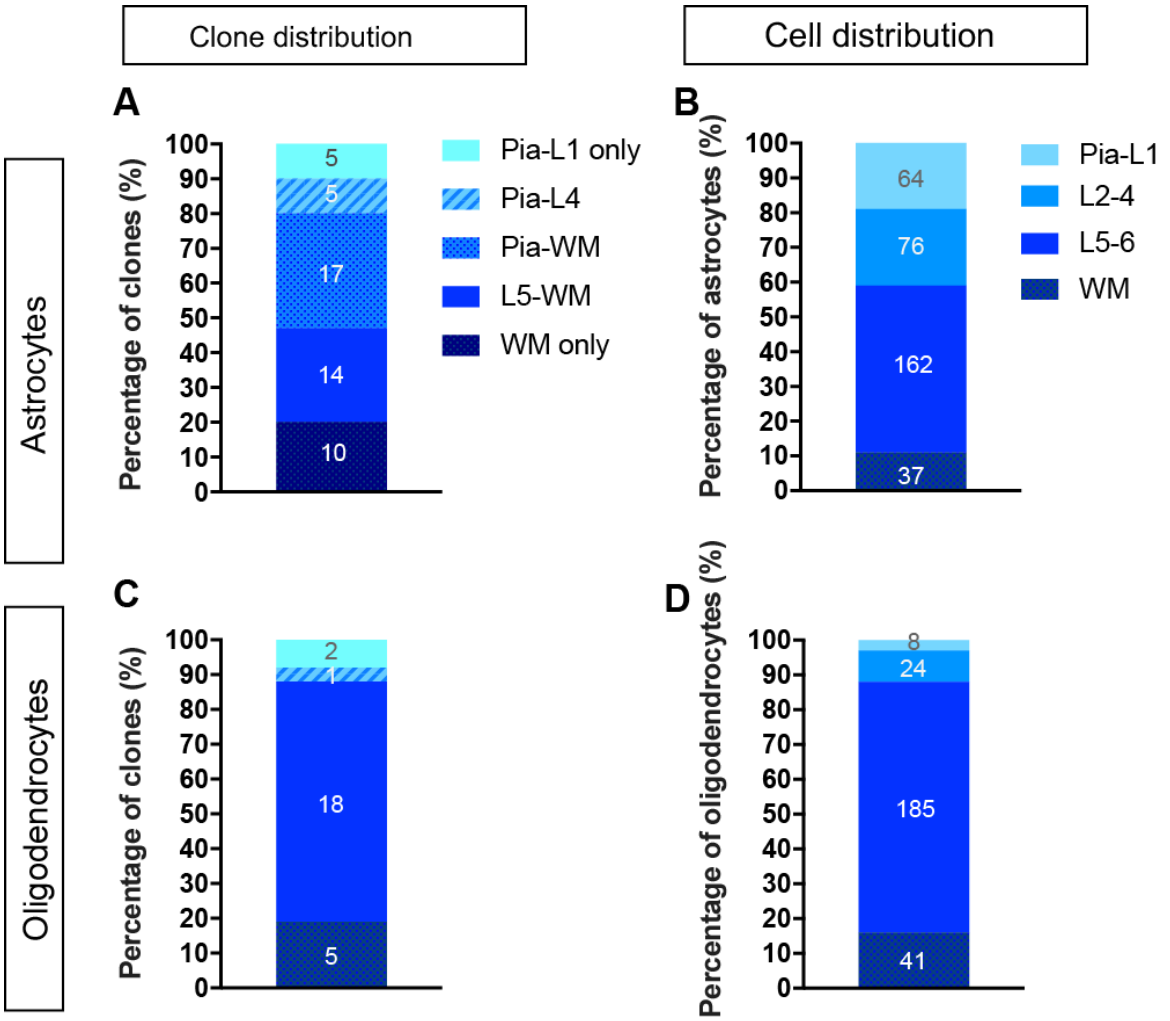

Figure 3.7 Laminar distribution of glia generated by mixed neuron/glia clones. (A) 3D reconstructions of mixed clones containing astrocytes and oligodendrocytes. Lamina are indicated with colored lines, following borders shown by DAPI signal. **(B)** Laminar distribution of oligodendrocytes in mixed clones containing oligodendrocytes. **(C)** Laminar distribution of all oligodendrocytes recovered in mixed clones. **(D)** Laminar distribution of astrocytes in mixed clones containing astrocytes. **(E)** Laminar distribution of all astrocytes recovered in mixed clones. For N+A+O clones, astrocyte and oligodendrocyte lineages were examined separately.

Chapter 4

Discussion and Future Directions

4.1 Clonal analysis of RGPs reveals several aspects of how cortical gliogenesis is regulated at the individual progenitor level

Proper neural function relies on the regulation of the number and proportion of neuronal and non-neuronal cell types. To understand how individual progenitor behavior is regulated to establish the correct numbers, subtypes, and arrangements of the glial population, we performed clonal analysis of neocortical RGPs at their transition from neurogenesis into gliogenesis. Our work is the first to examine lineage relationships between the three major neural cell types – neurons, astrocytes, and oligodendrocytes. Further, our work is the first to trace gliogenic RGPs in a progenitor domain and time-specific manner. This work is the first to examine gliogenesis at the individual progenitor resolution which such specificity and resolution.

To summarize our key findings: after neocortical RGPs enter the asymmetric neurogenic division stage, around E13, we found that glial output is not correlated with embryonic induction time nor neuron output. This result suggests that the regulation of

glia number is independent of when exit from neurogenesis occurs. We found three different RGP types based on their potential to make neurons, astrocytes, and/or oligodendrocytes. These subtypes are equally distributed throughout late embryonic induction timepoints and neocortical brain regions, suggesting a general mechanism for determining RGP subtype. We found a tripotent progenitor (N+A+O) capable of making twice the glia of their bipotent counterparts (N+A, N+O). Our results also suggest a fixed rate at which RGPs, which represent a temporally uncoordinated population, exit neurogenesis and transition into gliogenesis.

We found that *Emx1*-RGP oligodendrogenesis contrasts with astrogliogenesis in several aspects. Consistent with previously published data based on tracing *Thy1.2*-Cre progenitors[79], a promoter that labels RGPs nonspecifically, we found that *Emx1* RGP-derived astrocytes account for most of the neocortical astrocytes. However, our data suggests that at least 30% of oligodendrocytes emerge from a different progenitor domain. The decline of the *Emx1*-derived oligodendrocyte population has been reported[62]. We found that OPCs have a higher proliferative capacity than astrocyte-restricted precursors. Finally, our results were the first to analyze at the clonal level RGP-derived glia are allocated to the cortex – possibly providing insight into developmental sources of glial heterogeneity. We found that the majority of

oligodendrocytes are clustered to one layer while astrocytes can span the full cortical width. Our data suggest separate lineages for Layer-1 and WM astrocytes, and suggests an inside-out allocation of astrocytes. Most oligodendrocytes are destined for deep cortical layers (5-6) and WM whereas 40% of astrocytes are destined for superficial layers (1-4). Further work, where population analysis and stereology is performed on the *Emx1*-derived glial population can reveal whether our findings at the individual progenitor level correspond to the number and distribution of astrocytes and oligodendrocytes throughout the neocortex.

The conclusions from this analysis point towards the importance of cell-intrinsic regulation in gliogenesis. We found a constant number of glia produced by progenitors labeled from E13 to E16, after most RGPs have entered asymmetric division. In these clones, we found no correlation between neuronal and glial output. These results indicate when we capture neurogenic phase of RGPs we can capture their full gliogenic potential. This is in accordance the established sequence that gliogenesis precedes neurogenesis in RGPs. Further, these data suggest that there is a regulation in the number of glia produced by an individual RGP independent from when exit from neurogenesis occurs. The proportion and glial output of different RGP types are consistent throughout neocortical brain regions and induction time points. This

suggests specification of RGP subtypes is independent of developmental stage and location along the anterior-posterior axis, but is a general property.

Glial output is also independent of developmental time and neocortical region, which also points toward the importance of a cell-intrinsic mechanism in the determination of glial output. Extracellular signal availability varies according to brain region and developmental time. Morphogens such as Shh and BMP, which have been demonstrated to impact gliogenesis have a temporal and regional gradient[85]. In addition, extracellular cues such as cytokines that are available vary through developmental time as the nascent cortical plate is invaded by newly born neurons[86]. Further, we see that the oligodendrocyte and astrocyte output of glial progenitors are not a factor of the progenitor's potential to produce different cell types.

MADM-based clonal analysis of neocortical gliogenesis uncovered three distinct clone types based on their capacity to make neurons (N), astrocytes (A), and/or oligodendrocytes (O); based on their composition, these types are N+A, N+O, and N+A+O. That we uncovered clones that only have astrocytes or oligodendrocytes and clones that have both glial subtypes indicates that not all progenitors need to undergo a sequence of making one glial subtype prior to making the other, but may be restricted

to producing one type of glia. Had their been common gliogenic sequence for all progenitors we would expect to uncover either N+O and N+A+O clones, while clones containing astrocytes are devoid of neurons; or N+A clones and N+A+O clones, with oligodendrocyte clones. Tri-potent (N+A+O) progenitors produce on average twice as much glia but the same number of individual glial types compared to their bi-potent (N+A, N+O) counterparts. We found no correlation between the astrocyte and oligodendrocyte output of N+A+O clones. This suggests that oligodendrocyte and astrocyte precursors that arise from an individual RGP maintain their intrinsic proliferative potential. The increased proliferation potential and ability to produce cell types in N+A+O clones may suggest that the increased capacity to specify cell types is a factor of increased duration in cell cycle. Analysis of MADM labeled clones at early postnatal stages, where gliogenesis largely occurs, would increase our resolution into how glia clones are established. Combining the data of developing clones with our data of mature clones in the adult brain will offer snapshots to help decipher the sequence of gliogenesis and distribution of glial cells.

Comparison of the fraction of single-neuron gliogenic clones at different time point shows that a similar proportion of clones transition out of neurogenesis across the analyzed late embryonic stages (E13-E15). This suggests a fixed rate at which RGPs,

which represent a temporally uncoordinated population, exit neurogenesis and transition into gliogenesis. Most gliogenic RGPs proceed to produce glia after a final neurogenic division, however we found two special cases:

(1) RGPs produce a glial precursor and continue to produce neurons before entering gliogenesis. This result suggests that gliogenesis may occur concurrently with neurogenesis from the same parent RGP. That is, there is not a molecular on/off switch that occurs at the start of gliogenesis, but a program that can also lead to the production of neurons.

(2) One of the daughter cells of the RGP is lost, while the RGP continues to produce cells. This result will be discussed more in depth in section 6.2.

Analysis of differentiation potential in single neuron gliogenic clones shows that the majority of RGPs (63.2%) produce neurons and astrocytes, approximately one third make all three cell types (26.3 %), and 1 in 10 (10.5%) are restricted to the production of neurons and oligodendrocytes. We can combine our quantitative results to estimate the proportion of neurons and glia in the neocortex:

$$\frac{Fraction\ gliogenic\ RGPs * ((Avg.N\ Astrocytes)(Fraction\ astrogenic\ RGPs) + (Avg.N\ oligodendrocytes)(Fraction\ oligodendrogenic\ RGPs))}{RGP\ neuron\ unitary\ output}$$

Where the fraction of gliogenic RGPs is 1/6, average number of astrocytes is 7.2, fraction astrogenic RGPs is 89.5/100, average number of oligodendrocytes is 10.3, and the fraction of oligodendrogenic clones is 36.8/100.

We find that the overall ratio of glia to neurons is 1:5. Our glia:neuron ratio is much lower than the estimated 56.2% of non-neuronal cells in the mouse cortex (Herculano-Houzel 2006). This result suggests that roughly 30% of neocortical glia are derived from a source other than *Emx1*+ progenitors, which are the exclusive source of neocortical pyramidal neurons. These additional glia could possibly arise from a pool of glia-restricted precursors in the dorsal VZ/SVZ, or migration of cells from other developmental niches. The astrocyte to neuron ratio calculated by the above formula is 1:7.7. This ratio is similar to previously published estimates, where the ratio in lineage-traced neocortical columns was 1:7.4. Similarly, they found a 1:8.4 S100B+/NeuN ratio across the gray matter. This suggests that most neocortical astrocytes arise from *Emx1*+ progenitors.

The oligodendrocyte:neuron ratio based on our clonal analysis data is 1:14.2. Estimates of oligodendrocyte number is the cortex are unavailable, however data collected through our method can only be an underestimate of oligodendrocytes in the

neocortex. Fate mapping experiments have estimated that by adult stages the contribution to cortical oligodendrocytes from *Emx1*+ progenitors falls from 70% at early postnatal stages to 30%. This indicates that the oligodendrocyte population comes in large part from sources other than neocortical RGPs.

The frequency distributions of clone sizes for astrocytes and oligodendrocytes differ. About 10% of clones with astrocytes produce only one astrocyte. However, all clones containing oligodendrocytes produced 2 or more oligodendrocytes. When we examine the frequency distribution of different clone sizes, we find similar frequencies of clone sizes, with a much smaller probability for larger clones. For oligodendrocytes, there seems to be a bimodal distribution, with one curve describing the probabilities of smaller clones 1-8 and another curve describing larger clone sizes 13-24. These data suggest different programs regulate the proliferation of astrocyte-restricted and oligodendrocyte-restricted glial precursors. Because OPCs remain proliferative through adulthood, it is possible that larger oligodendrocyte clone sizes are a product of progenitors that divide throughout the animal's lifespan, or whether this is directly a product of late embryonic/early postnatal development. It would be interesting to examine how clone size and distribution is established through developmental timepoints, from the onset of gliogenesis (~E16) to adulthood, by performing clonal

analysis with endpoints through the animal's life and comparing data acquired from different endpoints.

Most oligodendrocyte clones (77.8%) are clustered into a single lamina. These single layer clones are mostly found in layer 6. This is compared to astrocytes, where a smaller fraction (36%), are restricted to a single layer. Astrocytes clones that span a single layer are mostly found in the white matter. Because white matter astrocytes are of the fibrous subtype, this result suggest that fibrous astrocytes have a diminished proliferative capacity compared to protoplasmic and 'fibroblast-like' astrocytes.
For clones where glia spans multiple layers, we see a wider spread in the distribution of astrocytes compared to that of oligodendrocytes Oligodendrocyte clones are mostly distributed in deep cortical layers and white matter. This contrasts with the distribution of astrocytes where 41.1% of total recovered astrocytes are destined for layers spanning the pial surface to layer 4. Together these results are consistent with an even distribution of astrocytes throughout the neocortical parenchyma, in contrast with a higher concentration of oligodendrocytes in deep cortical layers and white matter.

4.2 Effects of postnatal experience in neocortical gliogenesis

Although there is limited neurogenesis at postnatal ages, the glial population reaches its proliferation peak postnatally and continues into adult stages. This postnatal plasticity is amenable to the experience of the animal. It has been demonstrated that interventions such as environmental enrichment and motor learning may promote gliogenesis in task-specific regions such as mPFC, cingulate cortex, motor cortex, and visual cortex[87]. It has been demonstrated in human that skill learning can increase white matter regions[88].

Environmental enrichment protocols vary but include the introduction of novel toys, tunnels, food, and running wheel into grouped housed rodent cages. This leads to increased motor and cognitive activity and in turn, increased proliferation of oligodendrocytes. This proliferation may be mediated through increased neural activity as it has been demonstrated that stimulation of neurons promotes oligodendrogenesis and increases myelination in a circuit-specific manner[36].

Negative events may also shape cortical architecture. Stress, through either maternal stress or social isolation is thought to negatively affect oligodendrogenesis. This may be mediated by an increased release of stress-response hormones such as

corticosterone. Corticosteroids have shown to decrease OPC proliferation and myelin production[89].

By performing clonal analysis in animals housed under different conditions such as an enriched environment or social isolation, we can determine at the individual RGP level how proliferation is regulated in response to postnatal experience. How is clone size affected? Are certain RGP subtypes more susceptible to proliferate? Which glial lineages are affected? This research has important implications for future developmental studies. It may contribute to the body of work that demonstrates that animal conditions, such as maternal behavior, social interactions, environment may confound research.

4.3 Contribution of cell death in shaping neocortical cell population

Development and maintenance of the cell population in a tissue is a balance between the generation of new cells and the removal of unnecessary cells. During nervous tissue development, transient cell populations are lost as they exit cell cycle. Oligodendrocytes that invade the neocortex, during the first wave of oligodendrogenesis, invade the cortex form the ventral progenitor domain of Nkx2.1 progenitors. Nkx2.1-derived neocortical oligodendrocytes are removed through

caspase-3 dependent cell death by the time the two subsequent waves of oligodendrocytes populate the neocortex, derived from Dlx2 and Emx1 domains.

Cell death also occurs in the neuronal lineage. About 40% of developing interneuron population in the cortex is also removed through apoptosis[90]. Interneuron death is mediated by Bax (Bcl-2 asssociated X) – dependent apoptosis in postnatal stages. In Bax mutants, cell death of GAD67-GFP interneurons was nearly absent[91]. Bax is a protein that mediates cell death by inserting itself in the mitochondria in response to a variety of stress signals. In response to signaling, Bax changes conformation and becomes a pore-forming protein which induces apoptosis through release of cytochrome C and other mitochondrial proteins into the cytosol. Recent studies indicate that there is reduction in the number of neocortical excitatory neurons between P2 and P5, with the population dropping approximately 12% between these postnatal development stages, and then remaining stable into adulthood.[84]

How does apoptosis help sculpt the development of the cortical cell population? One caveat of our clonal analysis is that the total number of glia recovered in our MADM-labeled clones may not be equal to the total number of glia that a labeled progenitor produces. About 30% of clones were composed of neurons and the glia in

one color. This strongly suggests, that at the time of mitosis where the parent RGP was labeled, the second daughter lineage underwent cell death.

Clonal and population resolution studies can help elucidate the contribution of cell death in the neocortex. Bax mutation has been linked to developmental apoptosis in the neocortex. However, the contribution of Bax-mediated cell death in the *Emx-1* glial lineage has not been directly examined. To analyze the role of Bax-mediated cell death in shaping the neocortical cell population, we may quantify and compare the number of pyramidal neurons, astrocytes, and oligodendrocytes in wild type, heterozygous, and Bax mutant animals. Emx1-derived cells can be distinguished from the general population by lineage tracing Emx1 progenitors with a Cre-driven by the Emx1 promoter combined with a loxP flanked allele of a fluorescent protein such as eGFP. To examine the effect of Bax deletion on individual RGPs, clonal analysis can be performed by combining the Emx1-MADM system with a Bax mutant background. Bax can be bred into the Emx1-MADM-TG animals and the Emx1-MADM-GT allele to generate Emx1-MADM-TG/GT Bax-/-. Clone size and composition can be compared between mutant animals and their Bax heterozygous littermates.

Chapter 5

Methods & Materials

5.1 Animals and clonal induction

MADM-11^{GT} (JAX Stock No. 013749) and MADM-11^{TG} (JAX Stock No. 013751) mice were produced as previously described[82]. Emx1-CreER^{T2} mice were kindly provided by Dr. Nicoletta Tekki-Kessaris. Mice were bred and maintained according to guidelines established by the Institutional Animal Care and Use Committee of Memorial Sloan Kettering Cancer Center. For MADM labeling, Emx1-CreER$^{T2+/-}$; MADM-11$^{GT/GT}$ mice were crossed with MADM-11$^{TG/TG}$ mice and the time of pregnancy was determined by the presence of the vaginal plug (E0, ~noon). For clone induction, pregnant females were injected intraperitoneally with TM (T5648, Sigma) dissolved in corn oil (C8267, Sigma) at E10, E11, E12 and E13 at a dose of 5-25 μg/g body weight; or orally gavaged with TM at E13, E14, E15, and E16 at a dose of 150-300 μg/g body weight.

5.2 Tissue processing

Both male and female mice were perfused intracardially with 4%

paraformaldehyde (PFA) in phosphate-buffered saline (PBS, pH 7.4). Brains were removed and post-fixed overnight at 4°C. Serial coronal sections of individual brains were prepared using a vibratome (Leica Microsystems). Tissue was serially sectioned into 70-100 μm sections. Thicker sections resulted in us capturing more complete morphologies of cells in individual sections compared to thinner sections. We enhanced the intrinsic signal of the expressed GFP and RFP via immunohistochemistry, using antibodies specific to each protein. The sections were mounted onto slides for analysis.

The following primary antibodies were used: chicken anti-GFP (1:1,000 dilution, GFP-1020, Aves Lab), rabbit anti-RFP (1:1,000 dilution, 600-401-379, Rockland), guinea pig anti-RFP (1:10,000 dilution, produced by the Songhai Shi lab), goat anti-GFAP (1:200, ab53554, Abcam), and rabbit anti-Olig2 (1:500, AB9610, Millipore). For GFAP, antigen retrieval was performed in brains fixed 6.5 hr in 4% PFA & followed by incubation in sodium citrate buffer (pH 6.0) at 80°C for 30 min. Sections were mounted on glass slides, imaged using confocal microscopy (FV1000, Olympus or LSM700, Zeiss) and slide scanner (NanoZoomer 2.0-HT, Hamamatsu Photonics).

5.3 3D reconstruction

Full brain scans were performed by either optical detection in an epifluorescent microscope or by scanning entire brains using Nanozoomer. Sections were reconstructed by manual tracing of outer borders using Neurolucida (MBF Bioscience). Neurons, astrocytes, and oligodendrocytes were distinguished based on their morphology and marker expression (See Section 2.4). Cells were represented as colored symbols (3-4 times the size of the cell body). Layer boundaries based on nuclear staining were also documented. Laminar boundaries were traced based on DAPI nuclear staining. To annotate brain regions, landmarks such as the lateral ventricles and the hippocampus were traced and used to identify location along the anterior-posterior axis based on the Allen Brain Atlas (http://mouse.brain-map.org/static/atlas). Consecutive brain sections were aligned manually based on outer boundaries, laminar, and landmark outlines.

5.4 Statistics

Statistical methods were used to predetermine sample sizes. Data collection and analysis were not randomized nor performed blind to the conditions of the

experiments. Data points were selected based on labeling (G_2-X clones, green/red color) and composition (combination of neurons and glia). Data are mean ± S.E.M., and statistical differences between two groups were determined using non-parametric Mann–Whitney tests, which assume a non-Gaussian distribution. Chi-square tests were used to compare proportions between groups in contingency analyses. Linear regression analysis was performed to test for correlation between two parameters on X-Y plots. Data distribution was not formally tested. Statistical significance was set at $p<0.05$. Exact p-values are provided in the figure legends.

REFERENCES

1. Herculano-Houzel S. The glia/neuron ratio: How it varies uniformly across brain structures and species and what that means for brain physiology and evolution. *Glia*. 2014;62(9):1377-1391. doi:10.1002/glia.22683

2. Pelvig DP, Pakkenberg H, Stark AK, Pakkenberg B. Neocortical glial cell numbers in human brains. *Neurobiol Aging*. 2008;29(11):1754-1762. doi:10.1016/j.neurobiolaging.2007.04.013

3. Alliot F, Godin I, Pessac B. Microglia derive from progenitors, originating from the yolk sac, and which proliferate in the brain. *Dev Brain Res*. 1999;117(2):145-152. doi:https://doi.org/10.1016/S0165-3806(99)00113-3

4. Rouach N, Koulakoff A, Abudara V, Willecke K, Giaume C. Astroglial Metabolic Networks Sustain Hippocampal Synaptic Transmission. *Science (80-)*. 2008;322(5907):1551 LP-1555. http://science.sciencemag.org/content/322/5907/1551.abstract.

5. Iadecola C, Nedergaard M. Glial regulation of the cerebral microvasculature. *Nat Neurosci*. 2007;10(11):1369-1376. doi:10.1038/nn2003

6. Ullian EM, Sapperstein SK, Christopherson KS, Barres BA. Control of Synapse

Number by Glia. *Science (80-)*. 2001;291(5504):657 LP-661. http://science.sciencemag.org/content/291/5504/657.abstract.

7. Beattie EC, Stellwagen D, Morishita W, et al. Control of Synaptic Strength by Glial TNFα. *Science (80-)*. 2002;295(5563):2282 LP-2285. http://science.sciencemag.org/content/295/5563/2282.abstract.

8. Crawford, Devon; Jiang, Xiaoping; Taylor, Amanda; Mennerick S. Astrocyte-derived thrombospondins mediate the development of hippocampal presynaptic plasticity in vitro. *J Neurosci*. 2012;32(38):13100–13110. doi:10.1523/JNEUROSCI.2604-12.2012. Astrocyte-derived

9. Chung W, Allen NJ, Eroglu C. Astrocytes Control Synapse Formation, Function, and Elimination. *Cold Spring Harb Perspect Biol*. 2015:1-18. doi:10.1101/cshperspect.a020370

10. Araque A, Parpura V, Sanzgiri RP, Haydon PG. Tripartite synapses: glia, the unacknowledged partner. *Trends Neurosci*. 1999;22(5):208-215. doi:10.1016/S0166-2236(98)01349-6

11. Parpura V, Basarsky TA, Liu F, Jeftinija K, Jeftinija S, Haydon PG. Glutamate-mediated astrocyte–neuron signalling. *Nature*. 1994;369:744.

http://dx.doi.org/10.1038/369744a0.

12. Guthrie PB, Knappenberger J, Segal M, Bennett M V, Charles AC, Kater SB. ATP released from astrocytes mediates glial calcium waves. *J Neurosci*. 1999;19(2):520-528.

13. Mothet J-P, Pollegioni L, Ouanounou G, Martineau M, Fossier P, Baux G. Glutamate receptor activation triggers a calcium-dependent and SNARE protein-dependent release of the gliotransmitter D-serine. *Proc Natl Acad Sci U S A*. 2005;102(15):5606-5611. doi:10.1073/pnas.0408483102

14. Volterra A, Meldolesi J. Astrocytes, from brain glue to communication elements: the revolution continues. *Nat Rev Neurosci*. 2005;6:626. http://dx.doi.org/10.1038/nrn1722.

15. Bushong EA, Martone ME, Jones YZ, Ellisman MH. Protoplasmic Astrocytes in CA1 Stratum Radiatum Occupy Separate Anatomical Domains. *J Neurosci*. 2002;22(1):183-192.

16. Halassa MM, Fellin T, Takano H, Dong J-H, Haydon PG. Synaptic islands defined by the territory of a single astrocyte. *J Neurosci*. 2007;27(24):6473-6477. doi:10.1523/JNEUROSCI.1419-07.2007

17. Schummers J, Yu H, Sur M. Tuned Responses of Astrocytes and Their Influence on Hemodynamic Signals in the Visual Cortex. *Science (80-)*. 2008;320(5883):1638 LP-1643. http://science.sciencemag.org/content/320/5883/1638.abstract.

18. Padmashri R, Suresh A, Boska MD, Dunaevsky A. Motor-Skill Learning Is Dependent on Astrocytic Activity. 2015;2015.

19. Carlos M, Marcello M, Ainara V, Fiorenzo C. Increased expression of the astrocytic glutamate transporter GLT-1 in the prefrontal cortex of schizophrenics. *Glia*. 2004;49(3):451-455. doi:10.1002/glia.20119

20. Aida T, Yoshida J, Nomura M, et al. Astroglial Glutamate Transporter Deficiency Increases Synaptic Excitability and Leads to Pathological Repetitive Behaviors in Mice. *Neuropsychopharmacology*. 2015;40:1569. http://dx.doi.org/10.1038/npp.2015.26.

21. Jacobs S, Doering LC. Astrocytes Prevent Abnormal Neuronal Development in the Fragile X Mouse. *J Neurosci*. 2010;30(12):4508 LP-4514. http://www.jneurosci.org/content/30/12/4508.abstract.

22. Cox SB, Woolsey T a, Rovainen CM. Localized dynamic changes in cortical blood flow with whisker stimulation corresponds to matched vascular and neuronal

architecture of rat barrels. *J Cereb Blood Flow Metab*. 1993;13(6):899-913. doi:10.1038/jcbfm.1993.113

23. Mathiisen TM, Lehre KP, Danbolt NC, Ottersen OP. The perivascular astroglial sheath provides a complete covering of the brain microvessels: an electron microscopic 3D reconstruction. *Glia*. 2010;58(9):1094-1103. doi:10.1002/glia.20990

24. García-Marqués J, López-Mascaraque L. Clonal identity determines astrocyte cortical heterogeneity. *Cereb Cortex*. 2013;23(6):1463-1472. doi:10.1093/cercor/bhs134

25. Bardehle S, Krüger M, Buggenthin F, et al. Live imaging of astrocyte responses to acute injury reveals selective juxtavascular proliferation. *Nat Neurosci*. 2013;16(5):580-586. doi:10.1038/nn.3371

26. Martín-López E, García-Marques J, Núñez-Llaves R, López-Mascaraque L. Clonal astrocytic response to cortical injury. *PLoS One*. 2013;8(9):e74039. doi:10.1371/journal.pone.0074039

27. Emsley J, Macklis J. Astroglial heterogeneity closely reflects the neuronal-defined anatomy of the adult murine CNS. *Neuron Glia Biol*. 2006;2(3):175-186. http://europepmc.org/articles/PMC1820889. Accessed May 13, 2014.

28. Zeisel A, Hochgerner H, Lonnerberg P, et al. Molecular architecture of the mouse nervous system. *bioRxiv*. January 2018. http://biorxiv.org/content/early/2018/04/06/294918.abstract.

29. Garcia a DR, Petrova R, Eng L, Joyner AL. Sonic hedgehog regulates discrete populations of astrocytes in the adult mouse forebrain. *J Neurosci*. 2010;30(41):13597-13608. doi:10.1523/JNEUROSCI.0830-10.2010

30. Sosunov A a, Wu X, Tsankova NM, Guilfoyle E, McKhann GM, Goldman JE. Phenotypic heterogeneity and plasticity of isocortical and hippocampal astrocytes in the human brain. *J Neurosci*. 2014;34(6):2285-2298. doi:10.1523/JNEUROSCI.4037-13.2014

31. Tang X, Taniguchi K, Kofuji P. HETEROGENEITY OF KIR4.1 CHANNEL EXPRESSION IN GLIA REVEALED BY MOUSE TRANSGENESIS. *Glia*. 2009;57(16):1706-1715. doi:10.1002/glia.20882

32. Marín-padilla M. Prenatal development of fibrous (white matter), protoplasmic (gray matter), and layer I astrocytes in the human cerebral cortex: A Golgi study. *J Comp Neurol*. 1995;357(4):554-572. doi:10.1002/cne.903570407

33. Colombo JA, Reisin HD. Interlaminar astroglia of the cerebral cortex: a marker of

the primate brain. *Brain Res*. 2004;1006(1):126-131. doi:10.1016/j.brainres.2004.02.003

34. Oberheim NA, Takano T, Han X, et al. Uniquely hominid features of adult human astrocytes. *J Neurosci*. 2009;29(10):3276. doi:10.1523/JNEUROSCI.4707-08.2009

35. Purves D, Augustine GJ, Fitzpatrick D, et al. editors. Increased Conduction Velocity as a Result of Myelination. In: *Neuroscience*. 2nd editio. Sunderland (MA): Sinauer Associates; 2001:Available from: https://www.ncbi.nlm.nih.gov/books.

36. Gibson EM, Purger D, Mount CW, et al. Neuronal Activity Promotes Oligodendrogenesis and Adaptive Myelination in the Mammalian Brain. *Science*. 2014;344(6183):1252304. doi:10.1126/science.1252304

37. Lee Y, Morrison BM, Li Y, et al. Oligodendroglia metabolically support axons and contribute to neurodegeneration. *Nature*. 2012;487(7408):443-448. doi:10.1038/nature11314

38. Hughes EG, Kang SH, Fukaya M, Bergles DE. Oligodendrocyte progenitors balance growth with self-repulsion to achieve homeostasis in the adult brain. *Nat Neurosci*. 2013;16(6):668-676. doi:10.1038/nn.3390

39. Wenhui H, Na Z, Xianshu B, et al. Novel NG2-CreERT2 knock-in mice

demonstrate heterogeneous differentiation potential of NG2 glia during development. *Glia*. 2014;62(6):896-913. doi:10.1002/glia.22648

40. Marques S, Zeisel A, Codeluppi S, et al. Oligodendrocyte heterogeneity in the mouse juvenile and adult central nervous system. *Science (80-)*. 2016;352(6291):1326 LP-1329. http://science.sciencemag.org/content/352/6291/1326.abstract.

41. Zhu X, Bergles DE, Nishiyama A. NG2 cells generate both oligodendrocytes and gray matter astrocytes. *Development*. 2008;135(1):145 LP-157. http://dev.biologists.org/content/135/1/145.abstract.

42. Chittajallu R, Aguirre A, Gallo V. NG2-positive cells in the mouse white and grey matter display distinct physiological properties. *J Physiol*. 2004;561(Pt 1):109-122. doi:10.1113/jphysiol.2004.074252

43. Dimou L, Simon C, Kirchhoff F, Takebayashi H, Götz M. Progeny of Olig2-Expressing Progenitors in the Gray and White Matter of the Adult Mouse Cerebral Cortex. *J Neurosci*. 2008;28(41):10434 LP-10442. http://www.jneurosci.org/content/28/41/10434.abstract.

44. Rakic P. Specification of cerebral cortical areas. *Science*. 1988;241(4862):170-176.

doi:10.1126/science.3291116

45. Rakic P. Developmental and evolutionary adaptations of cortical radial glia. *Cereb Cortex*. 2003;13(6):541-549. http://www.ncbi.nlm.nih.gov/pubmed/12764027.

46. Hatten ME. Central Nervous System Neuronal Migration. *Annu Rev Neurosci*. 1999;22(1):511-539. doi:10.1146/annurev.neuro.22.1.511

47. Gao P, Postiglione MP, Krieger TG, et al. Deterministic progenitor behavior and unitary production of neurons in the neocortex. *Cell*. 2014. doi:10.1016/j.cell.2014.10.027

48. Marin-Padilla M. Prenatal and early postnatal ontogenesis of the human motor cortex: A Golgi study. I. The sequential development of the cortical layers. *Brain Res*. 1970;23(2):167-183. doi:https://doi.org/10.1016/0006-8993(70)90037-5

49. Marin-Padilla M. Early prenatal ontogenesis of the cerebral cortex (neocortex) of the cat (Felis domestica). A Golgi study. *Z Anat Entwicklungsgesch*. 1971;134(2):117-145. doi:10.1007/BF00519296

50. Anthony TE, Klein C, Fishell G, Heintz N. Radial Glia Serve as Neuronal Progenitors in All Regions of the Central Nervous System. *Neuron*. 2004;41(6):881-890. doi:10.1016/S0896-6273(04)00140-0

51. Malatesta P, Hack M a., Hartfuss E, et al. Neuronal or Glial ProgenyRegional Differences in Radial Glia Fate. *Neuron*. 2003;37:751-764. doi:10.1016/S0896-6273(03)00116-8

52. Malatesta P, Hartfuss E, Götz M. Isolation of radial glial cells by fluorescent-activated cell sorting reveals a neuronal lineage. *Development*. 2000;127(24):5253-5263. http://www.ncbi.nlm.nih.gov/pubmed/11076748.

53. Noctor SC, Flint AC, Weissman TA, Dammerman RS, Kriegstein AR. Neurons derived from radial glial cells establish radial units in neocortex. *Nature*. 2001;409:714. http://dx.doi.org/10.1038/35055553.

54. Noctor SC, Martínez-Cerdeño V, Ivic L, Kriegstein AR. Cortical neurons arise in symmetric and asymmetric division zones and migrate through specific phases. *Nat Neurosci*. 2004;7(2):136-144. doi:10.1038/nn1172

55. Kowalczyk T, Pontious A, Englund C, et al. Intermediate Neuronal Progenitors (Basal Progenitors) Produce Pyramidal–Projection Neurons for All Layers of Cerebral Cortex. *Cereb Cortex (New York, NY)*. 2009;19(10):2439-2450. doi:10.1093/cercor/bhn260

56. Nadarajah B, Parnavelas JG. Modes of neuronal migration in the developing

cerebral cortex. *Nat Rev Neurosci*. 2002;3:423. http://dx.doi.org/10.1038/nrn845.

57. Mountcastle VB. The columnar organization of the neocortex. *Brain*. 1997;120(4):701-722. doi:10.1093/brain/120.4.701

58. Yu Y-C, Bultje RS, Wang X, Shi S-H. Specific synapses develop preferentially among sister excitatory neurons in the neocortex. *Nature*. 2009;458(7237):501-504.

59. Yu Y-C, He S, Chen S, et al. Preferential electrical coupling regulates lineage-dependent microcircuit assembly in the neocortex. *Nature*. 2012;486(7401):113-117. doi:10.1038/nature10958

60. Li Y, Lu H, Cheng P, et al. Clonally related visual cortical neurons show similar stimulus feature selectivity. *Nature*. 2012;486:118. http://dx.doi.org/10.1038/nature11110.

61. Tabata H. Diverse subtypes of astrocytes and their development during corticogenesis. *Front Neurosci*. 2015;9:114. doi:10.3389/fnins.2015.00114

62. Kessaris N, Fogarty M, Iannarelli P, Grist M, Wegner M, Richardson WD. Competing waves of oligodendrocytes in the forebrain and postnatal elimination of an embryonic lineage. *Nat Neurosci*. 2006;9(2):173-179. doi:10.1038/nn1620

63. Siddiqi F, Chen F, Aron AW, Fiondella CG, Patel K, LoTurco JJ. Fate mapping by piggybac transposase reveals that neocortical glast+ progenitors generate more astrocytes than nestin+ progenitors in rat neocortex. *Cereb Cortex*. 2014;24(2):508-520. doi:10.1093/cercor/bhs332

64. Deneen B, Ho R, Lukaszewicz A, Hochstim CJ, Gronostajski RM, Anderson DJ. The Transcription Factor NFIA Controls the Onset of Gliogenesis in the Developing Spinal Cord. *Neuron*. 2006;52(6):953-968. doi:10.1016/j.neuron.2006.11.019

65. Stolt CC, Lommes P, Sock E, Chaboissier M-C, Schedl A, Wegner M. The Sox9 transcription factor determines glial fate choice in the developing spinal cord. *Genes Dev*. 2003;17(13):1677-1689. doi:10.1101/gad.259003

66. Kang P, Lee HK, Glasgow SM, et al. Sox9 and NFIA Coordinate a Transcriptional Regulatory Cascade during the Initiation of Gliogenesis. *Neuron*. 2012;74(1):79-94. doi:10.1016/j.neuron.2012.01.024

67. Nagao M, Ogata T, Sawada Y, Gotoh Y. Zbtb20 promotes astrocytogenesis during neocortical development. *Nat Commun*. 2016;7:11102. http://dx.doi.org/10.1038/ncomms11102.

68. Rowitch DH, Kriegstein AR. Developmental genetics of vertebrate glial-cell specification. *Nature*. 2010;468(7321):214-222. doi:10.1038/nature09611

69. Freeman MR. Specification and morphogenesis of astrocytes. *Science*. 2010;330(6005):774-778. doi:10.1126/science.1190928

70. Namihira M, Nakashima K. Mechanisms of astrocytogenesis in the mammalian brain. *Curr Opin Neurobiol*. 2013;23(6):921-927. doi:https://doi.org/10.1016/j.conb.2013.06.002

71. Kamakura S, Oishi K, Yoshimatsu T, Nakafuku M, Masuyama N, Gotoh Y. Hes binding to STAT3 mediates crosstalk between Notch and JAK–STAT signalling. *Nat Cell Biol*. 2004;6:547. http://dx.doi.org/10.1038/ncb1138.

72. Barres BA, Hart IK, Coles HSR, et al. Cell death and control of cell survival in the oligodendrocyte lineage. *Cell*. 1992;70(1):31-46. doi:10.1016/0092-8674(92)90531-G

73. Bandeira F, Lent R, Herculano-Houzel S. Changing numbers of neuronal and non-neuronal cells underlie postnatal brain growth in the rat. *Proc Natl Acad Sci U S A*. 2009;106(33):14108-14113. doi:10.1073/pnas.0804650106

74. Tsai H-H, Li H, Fuentealba LC, et al. Regional Astrocyte Allocation Regulates CNS Synaptogenesis and Repair. *Science*. 2012;337(6092):358-362.

doi:10.1126/science.1222381

75. Zerlin M, Milosevic A, Goldman JE. Glial progenitors of the neonatal subventricular zone differentiate asynchronously, leading to spatial dispersion of glial clones and to the persistence of immature glia in the adult mammalian CNS. *Dev Biol*. 2004;270(1):200-213. doi:10.1016/j.ydbio.2004.02.024

76. Levison SW, Chuang C, Abramson BJ, Goldman JE. The migrational patterns and developmental fates of glial precursors in the rat subventricular zone are temporally regulated. *Development*. 1993;119(3):611-622. http://www.ncbi.nlm.nih.gov/pubmed/8187632.

77. Costa MR, Bucholz O, Schroeder T, Götz M. Late origin of glia-restricted progenitors in the developing mouse cerebral cortex. *Cereb Cortex*. 2009;19(July):135-143. doi:10.1093/cercor/bhp046

78. Ge W-P, Miyawaki A, Gage FH, Jan YN, Jan LY. Local generation of glia is a major astrocyte source in postnatal cortex. *Nature*. 2012;484(7394):376-380. doi:10.1038/nature10959

79. Magavi S, Friedmann D, Banks G, Stolfi A, Lois C. Coincident generation of pyramidal neurons and protoplasmic astrocytes in neocortical columns. *J*

Neurosci. 2012;32(14):4762-4772. doi:10.1523/JNEUROSCI.3560-11.2012

80. Zong H, Espinosa JS, Su HH, Muzumdar MD, Luo L. Mosaic analysis with double markers in mice. *Cell*. 2005;121(3):479-492. doi:10.1016/j.cell.2005.02.012

81. Liu C, Sage JC, Miller MR, et al. Mosaic analysis with double markers reveals tumor cell of origin in glioma. *Cell*. 2011;146(2):209-221. doi:10.1016/j.cell.2011.06.014

82. Hippenmeyer S, Youn YH, Moon HM, et al. Genetic mosaic dissection of Lis1 and Ndel1 in neuronal migration. *Neuron*. 2010;68(4):695-709. doi:10.1016/j.neuron.2010.09.027

83. Gao P, Postiglione MP, Krieger TG, et al. Deterministic Progenitor Behavior and Unitary Production of Neurons in the Neocortex. *Cell*. 2014;159(4):775-788. doi:10.1016/j.cell.2014.10.027

84. Wong FK, Bercsenyi K, Sreenivasan V, Portalés A, Fernández-Otero M, Marín O. Pyramidal cell regulation of interneuron survival sculpts cortical networks. *Nature*. 2018;557(7707):668-673. doi:10.1038/s41586-018-0139-6

85. Dessaud E, McMahon AP, Briscoe J. Pattern formation in the vertebrate neural tube: a sonic hedgehog morphogen-regulated transcriptional network.

Development. 2008;135(15):2489 LP-2503. http://dev.biologists.org/content/135/15/2489.abstract.

86. Barnabé-Heider F, Wasylnka J a., Fernandes KJL, et al. Evidence that embryonic neurons regulate the onset of cortical gliogenesis via cardiotrophin-1. *Neuron*. 2005;48(2):253-265. doi:10.1016/j.neuron.2005.08.037

87. Ehninger D, Kempermann G. *Regional Effects of Wheel Running and Environmental Enrichment on Cell Genesis and Microglia Proliferation in the Adult Murine Neocortex*. Vol 13.; 2003. doi:10.1093/cercor/13.8.845

88. Bengtsson SL, Nagy Z, Skare S, Forsman L, Forssberg H, Ullén F. Extensive piano practicing has regionally specific effects on white matter development. *Nat Neurosci*. 2005;8:1148. http://dx.doi.org/10.1038/nn1516.

89. M. CD, Chao Z, R. KM, F. BW, J.M. FR. Corticosteroids delay remyelination of experimental demyelination in the rodent central nervous system. *J Neurosci Res*. 2006;83(4):594-605. doi:10.1002/jnr.20763

90. Southwell DG, Paredes MF, Galvao RP, et al. Intrinsically determined cell death of developing cortical interneurons. *Nature*. 2012;491(7422):109-113. doi:10.1038/nature11523

91. Knudson CM, Tung KSK, Tourtellotte WG, Brown GAJ, Korsmeyer SJ. Bax-Deficient Mice with Lymphoid Hyperplasia and Male Germ Cell Death. *Science (80-)*. 1995;270(5233):96 LP-99. http://science.sciencemag.org/content/270/5233/96.abstract.